# NUMERICAL ANALYSIS AND PARAMETER STUDY OF A MECHANICAL DAMPER IN MACHINE TOOL

By

DONGKI WON

A THESIS PRESENTED TO THE GRADUATE SCHOOL
OF THE UNIVERSITY OF FLORIDA IN PARTIAL FULFILLMENT
OF THE REQUIREMENTS FOR THE DEGREE OF
MASTER OF SCIENCE

UNIVERSITY OF FLORIDA

2004

ACKNOWLEDGMENTS

The researcher would like to express his gratitude to Dr. Nam Ho Kim for his inspiration, support and guidance during this research. Thanks also go to other committee members Dr. John Ziegert and Dr. Raphael Haftka for their support and service on the author's advisory committee. Special thanks go Mr. Charles Stanislaus and the students in the design lab for their help in completing tasks associated with the research. Finally, the author wishes to thank his wife, parents, and other family members. Without their support and caring this work would not have been possible.

TABLE OF CONTENTS

page

LIST OF TABLES

LIST OF FIGURES

Abstract of Thesis Presented to the Graduate School
of the University of Florida in Partial Fulfillment of the
Requirements for the Degree of Master of Science

NUMERICAL ANALYSIS AND PARAMETER STUDY
OF A MECHANICAL DAMPER IN MACHINE TOOL

By

Dongki Won

May, 2004

Chair: Nam Ho Kim
Major Department: Mechanical and Aerospace Engineering

When an endmill is used in high-speed machining, chatter vibration of the tool can cause undesirable results. This vibration increases tool wear and leaves chatter marks on the cutting surface. To reduce the chatter vibration, a layered-beam damper is inserted into the hole at the center of the tool. The friction work done by the relative motion between the tool and damper reduces chatter vibration. The purpose of this research is to design and optimize the configuration of the damper to obtain the maximum damping effect.

The analytical method has been reviewed, which is based on the assumption of constant contact pressure and uniform deflection. For the numerical approach, nonlinear finite element analysis is employed to calculate the distribution of the contact pressure under the centrifugal and cutting forces. The analytical and numerical results are compared and discussed.

In order to identify the effect of the damper's configuration, two design variables are chosen: the inner radius of the damper and the number of slotted dampers. During the parameter study and optimization, the inner radius is varied from 1.5mm to 3.5mm and the number of slotted dampers is varied from 2 to 10.

Results show that the damping effect is maximum when the inner radius is 1.5mm and the number of slotted dampers is 5. However, this result depends on the operating condition. Thus, it is suggested to prepare a set of dampers and to apply the appropriate one for the optimum damping effect for a given operating condition.

# CHAPTER 1
# INTRODUCTION

Milling is widely used in many areas of manufacturing. Traditionally, milling has been regarded as a slow and costly process. Therefore, many efforts have been made to improve the efficiency of milling. The main limitation of milling is caused by the vibration of the machine tool and workpiece. As the speed and the power of milling are increased, it is very important to control vibration of the tool.

Two different kinds of vibration affect the cutting operation. The one is the self-excited (chatter) vibration at the high spindle speed, and the other is vibration at the critical natural frequency. This research is focused on the former, which produces a wavy surface during the milling operation, as shown in Fig.1-1.

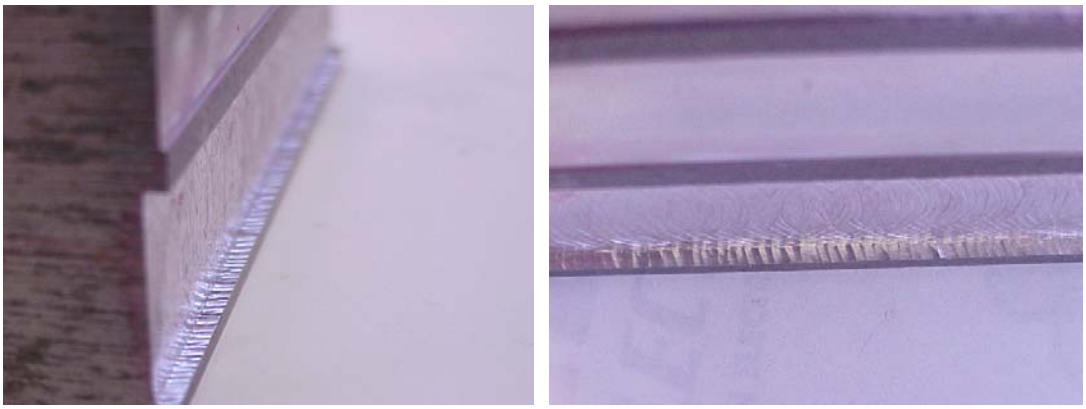

Figure 1-1. Chatter mark.

Various methods of preventing chatter have been incorporated into machine tool systems. In 1989, Cobb [2] developed dampers for boring bars. These dampers are composed of two different types. The first type, which Cobb calls a shear damper, has two end “caps” that fit snugly around a boring bar. Between these are sandwiched an

annular mass with plastic at each end, either in the form of ring or of several blocks at each end. This middle section of a mass and plastic pieces has a clearance from the boring bar, and is preloaded between the end caps with bolts. When the boring bar vibrates, the end caps transmit this vibration through the plastic pieces to the annular mass, which vibrates in tune. Since the plastic pieces do not slide on the faces of either one, a shear force is produced on the end faces of the plastic. The viscoelastic properties of the plastic provide damping for the system. The other type of damper proposed by Cobb is the compression damper in which the mass is again an annulus. This annulus is cut in half down its axis to form two half annuli. These are then bolted together around rings of plastic that are in contact with the boring bar. The bolts provide a preload on the plastic rings, and when the bar vibrates, the annular mass vibrates out of phase with it, compressing one side and then the other of the plastic rings. This alternate squeezing of the plastic creates damping, again by deforming the plastic, but in a compressive rather than shearing manner.

In 1998, Dean [3] focused on increasing the depth of cut and increasing axis federates to improve the metal removal rate (MRR). While he does not present any original ideas on chatter reduction, his thesis refers to work done by Smith [6] in which a chatter recognition system was developed. This system uses a microphone to detect the frequency of chatter when it occurs. The system then selects a different speed(according to the parameters of the system) and tries to machine again. This process repeats itself until chatter no longer occurs.

Much work in the field of structural damping has been done by Slocum [5]. In order to damp vibrations, Slocum uses layered beams with viscoelastic materials between

the layers. Two cantilevered beams are stacked on top of each other, and a force is applied to the end of the top beam. It is known that beams experience an axial shear force when displaced in this manner. Slocum's derivation calculates a relative displacement between corresponding points on the un-deformed beams. This is incorporated into a selfdamping structure by placing several small beams inside of a larger beam and injecting a viscoelastic material between them. This material bonds to each surface and thus, when there is a relative displacement, is deformed. The stretching of this material causes a dissipation of vibration energy and thus, damping.

In 2001, Sterling [7] explored the possibility of deploying a damper directly inside of a rotating tool. To reduce the chatter vibration, a layered-beam damper, which Sterling calls a finger, is inserted into the hole at the center of the tool. Due to the high-speed rotation, the outer surface of the damper contacts with the inner surface of the tool. When chatter vibration occurs, which is a deflection of the tool, work is done in the contact interface due to the friction force and the relative motion. This work is dissipative and reduces chatter vibration. He developed an analytical model and performed an experiment for the layered beam damper.

In this research, the work done by Sterling is further extended. Using finite element analysis, his analytical approach is compared to the numerical results. The objective of this research is to calculate the amount of friction work and to maximize its effect by changing the damper's configuration.

The organization of thesis is as follows. In Chapter 2, a simplified model of the endmill is introduced that can be used for analytical study and numerical simulation. In Chapter 3, the analytical approach is reviewed that qualitatively estimates the damping

work. Chapter 4 presents the background knowledge of finite element analysis in contact problems. Chapter 5 describes the numerical simulation procedure using the finite element method. Chapter 6 represents the parameter study according to the change of two design variables, followed by conclusions and future work at Chapter 7.

# CHAPTER 2
# SIMPLIFIED MODEL

The machine tool that we are considering in this research is a 4″ long endmill, as shown in Fig.2-1. Most endmills are of the solid beam type as shown in Fig.2-1 (a). In this type of tool, the only available damping mechanism is structural damping, which is very small. Structural damping, which is a variant of viscous damping, is usually caused by internal material friction. When the damping coefficient is small, as in the case of structures, damping is primarily effective at frequencies close to the resonant frequency of the structure.

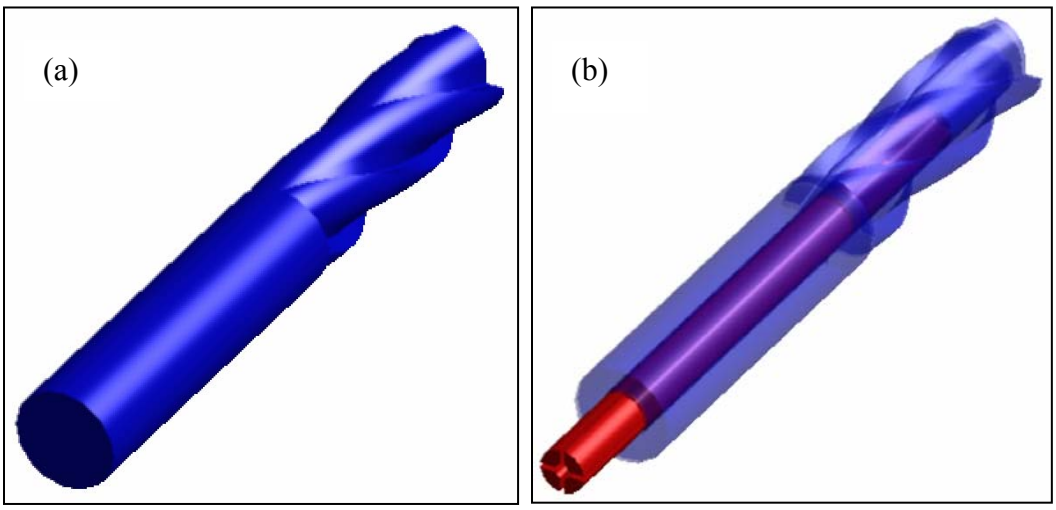


Figure 2-1. Endmill and damper. (a) the original solid endmill and (b) the damper inserted model

When a layered-beam damper (see Fig.2-1 (b)) is inserted into the hollow tool, the high-speed rotation causes a strong contact between the beam and tool. When chatter vibration occurs, it generates a relative motion between the beam and tool. Due to the contact force, this relative motion causes a friction force in the interface, which damps

the vibration. In this research, this damping mechanism will be referred to as a mechanical damper.

While the tool geometry is very important for cutting performance, the objective of this research is on the vibration of the tool. Thus, we want to simplfy the tool geometry so that the analytical and numerical studies in the following chapters will be convenient.

The first step of simplifying the endmill model is to suppress unnecessary geometric details, while maintaining the endmill's mechanical properties. The endmill model can be simplified as a cylinder because we are only interested in the contact surface, which is the inner surface of the tool. Fig.2-2 (b) illustrates the simplified model.

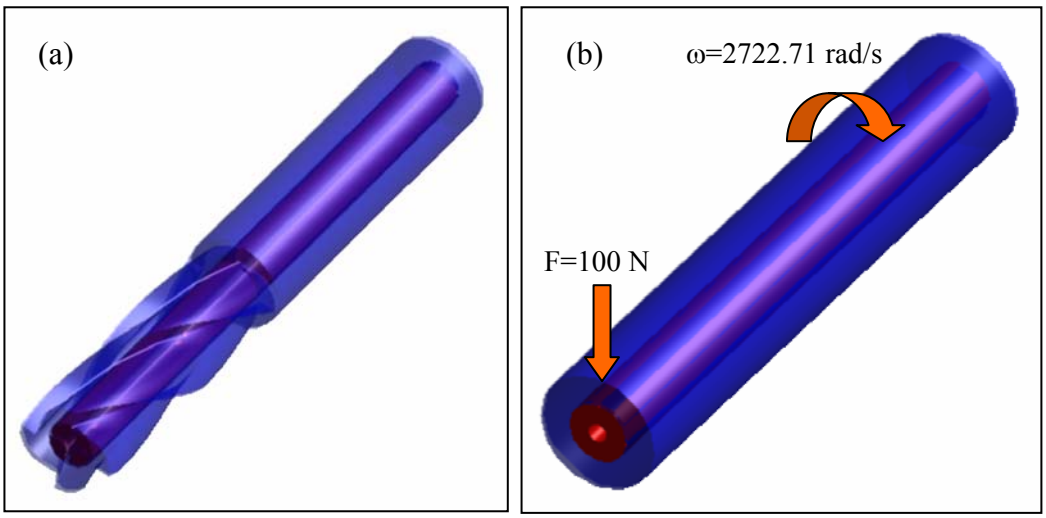


Figure 2-2. Model simplification. (a) the detailed tool model in which the damper is inserted and (b) the simplified model using hollowed cylinder.

The simplified endmill model is composed of two-hollowed cylinders. The outer cylinder represents the endmill tool, and the inner cylinder represents the damper. For convenience, the outer part (tool) is denoted as a shank, while the inner part (damper) is denoted as a finger. As schematically illustrated in Fig.2-3, the outer radius R1 of the finger is 1.5 mm, the inner radius R2 of the finger is 4.7625 mm, the inner radius R3 of the shank is 4.7625 mm, and the outer radius R4 of the shank is 9.525 mm. The length of

the endmill is 101.6mm. Because the gap between two contact surfaces is ignored, R2 is equal to R3. R1 will be varied from 1.0 mm to 3.5 mm during the parameter study in Chapter 6.

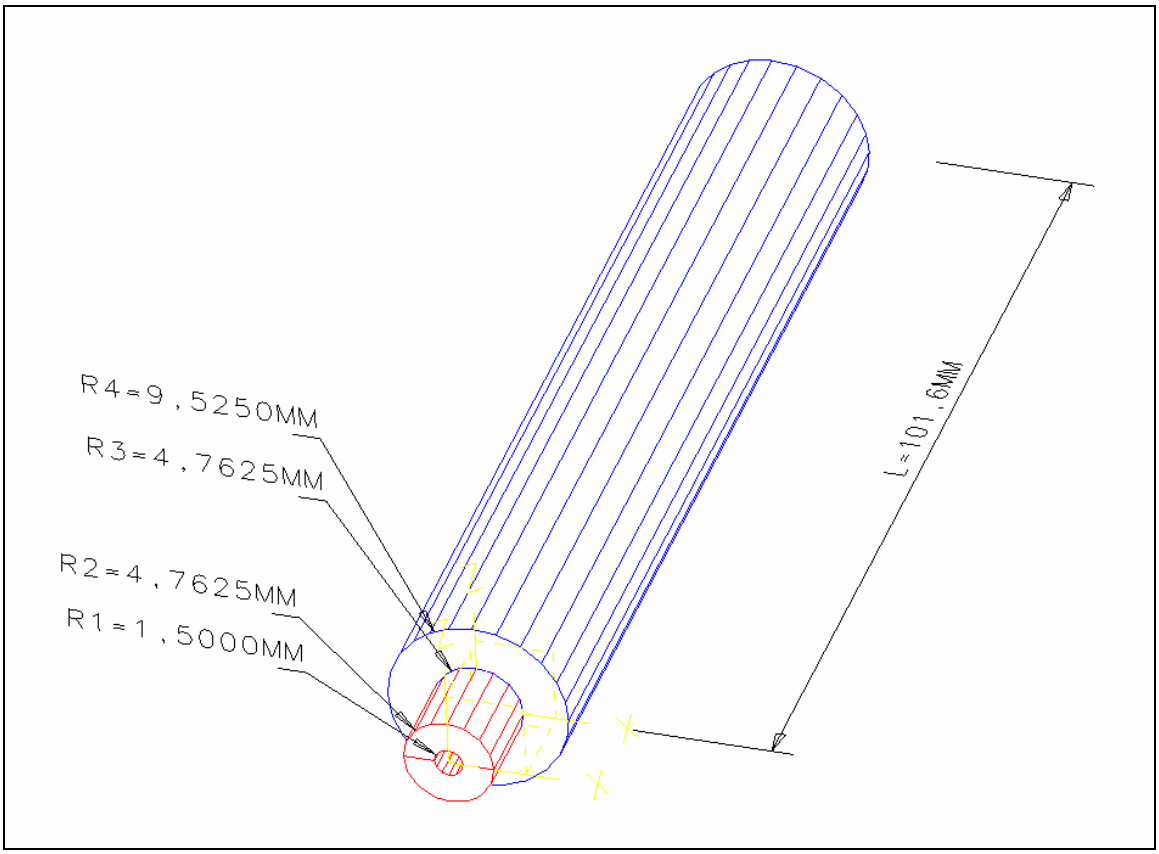


Figure 2-3. Dimensions of geometry.

Although Fig.2-3 shows only two fingers, the number of fingers can be altered to improve the damping performance. The parameter study in Chapter 6 will examine the effect of varying the number of fingers between 2 and 10. Because a damper with only one finger would have a lower contact pressure than the other cases, this case will not be considered.

Next, the operating condition is also simplified. The applied force is assumed to be sequential. It is first assumed that the tool is rotated with a constant angular velocity. The constant angular velocity will generate a constant contact force at the interface. For this

particular model, an angular velocity of 2,722.713rad/sec is used, which is equal to 26,000 rpm. In this initial state the endmill has not started cutting the surface. When the endmill starts cutting the surface, the tool undergoes a vertical force at the end of the endmill. To approximate the cutting process of the tool, a vertical force is applied at the tip. To accurately approximate the cutting force, the vertical force on the endmill needs to be measured and then an equal force needs be applied at the tip. However, since the objective of this research is vibration control, a representative force of 100N is applied. Thus, the damping work that will be calculated is not the actual magnitude, but rather a relative quantity.

For simplicity, the same material properties are assumed for both the shank and finger even though the stiffness of the finger is actually slightly higher than that of the shank. The material properties used are listed in Table 2-1.

Table 2-1. Material properties used for the shank and finger.

| Material Property | Value |
|---|---|
| Young's Modulus | 206780 MPa |
| Mass Density | $7.82\times10^{-9}$ ton/mm$^3$ |
| Friction Coefficient | 0.15 |

In the following chapters analytical and finite element analysis will use the simplified model to determine the conditions for maximum damping of the endmill.

# CHAPTER 3
# REVIEW OF ANALYTICAL APPROACH

It would be beneficial to review an analytical model before starting the finite element analysis because it will provide a qualitative estimation of the numerical approach. Sterling [7], a former researcher, developed an analytical method that can estimate the amount of friction work during chatter vibration. In this chapter, his analytical approach is reviewed and the results will be compared with finite element analysis results in Chapter 5.

The work done by the friction force that occurs between the inner surface of the endmill and the outer surface of the damper causes the damping effect that reduces the chatter vibration. According to the Coulomb friction model [9], the friction force and the damping work can be written as follows:

$$\begin{aligned} F_f &= \mu \times N \\ W_f &= F_f \times U_f \end{aligned} \tag{3.1}$$

where $F_f$ is the friction force, $\mu$ is the friction coefficient, $N$ is the normal contact force, $W_f$ is the friction work, and $U_f$ is the relative displacement between the two contact surfaces. The normal force $N$ is mainly caused by the centrifugal force created when the endmill is rotating. The relative displacement $U_f$ is mainly caused by the vertical deflection of the tool when the endmill starts cutting. Therefore, we can divide the endmill system into two states. The first state is when the endmill is rotating without any cutting operation. In this case, only the centrifugal force is applied. The second state is

when the endmill starts cutting. In this state, the vertical force is added at the tip of the endmill. Both the centrifugal force and the vertical force are applied in this state. If we assume that there is no relative motion in the first state, then we can calculate the work done by the friction force during the second state.

**Calculation of the Normal Force and the Contact Pressure**

In this section, the normal force and pressure that are caused by the rotational motion of the tool will be calculated. There are three assumptions for the analytical method in this step. Those are listed as below.

- There is no angular acceleration, which means the angular velocity is constant.
- There is no relative motion between the two contact surfaces during the first step, which means there is no slip in the contact surface during the rotational motion.
- Contact occurs throughout the entire contact area during the second state. In the actual case, contact may not occur in some portions of the interface. For example there will be no contact near the fixed end or on the two sides where the neutral axis lies. All of these effects are ignored, and it is assumed that contact occurs throughout the entire area.

Due to the second assumption, the contact pressure is calculated using the centrifugal force only and is assumed to remain constant. Now let us consider the simplified model, which was developed in Chapter 2 (Fig.2-3). The shank and the finger are hollowed cylinders. For simplicity, we only consider the case of a two-finger configuration. Figure 3-1 (a) shows the cross-sectional area and dimensions of the endmill system in which two fingers are inserted. Considering the symmetric geometry of the fingers, we can consider one finger, which is illustrated in Fig.3-1 (b). Since the finger can have an arbitrary location, $\theta$ represents the start angle of the finger. The point *G* indicates the first moment (centroid) of the finger's cross section, and *R* is the distance

between the center of the tool and the centroid *G*. The normal force *N* and contact pressure $P_c$ can then be obtained as,

$$N = MR\omega^2, \qquad P_c = \frac{MR\omega^2}{A_c} \tag{3.2}$$

where $A_c$ is the contact surface area, $M$ is the mass of the finger, and $\omega$ is the angular velocity. The first step of calculating the contact pressure is to calculate the distance *R*, which is determined by the centroid of the finger's cross section.

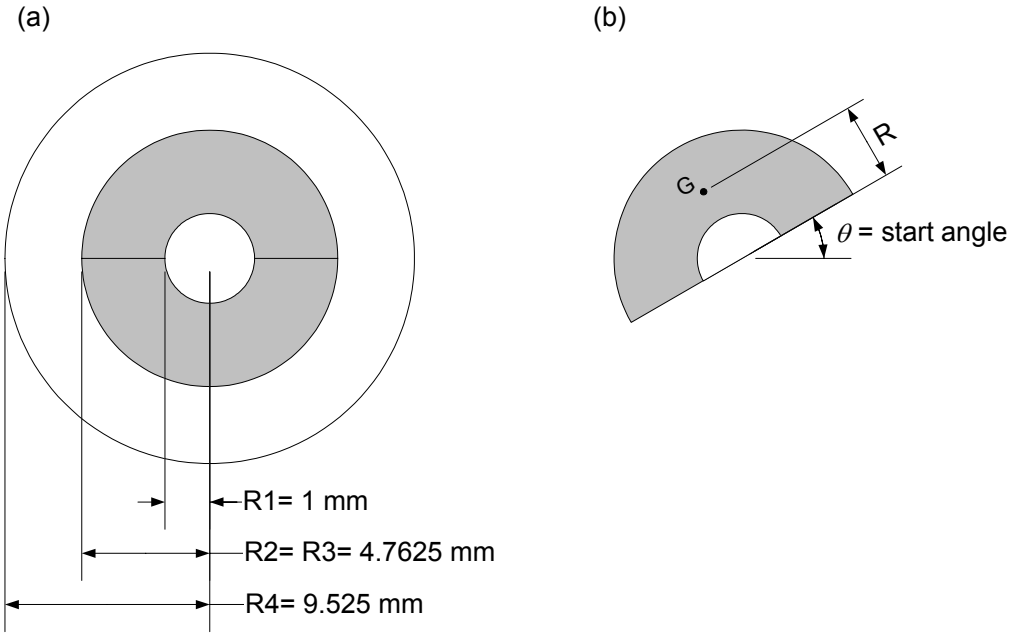


Figure 3-1. Cross sectional area of the endmill system. (a) Cross sectional area and dimension of the original model in which two fingers are inserted. (b) Cross sectional area of the finger. *G* is the mass center of the cross section, and $\theta$ is the start angle.

The centroid (first moment) of an assemblage of *n* similar quantities, $\Delta_1$, $\Delta_2$, $\Delta_3$, …, $\Delta_n$ situated at point $P_1$, $P_2$, $P_3$,…, $P_n$ for which the position vectors relative to a selected point O are $\mathbf{r}_1$, $\mathbf{r}_2$, $\mathbf{r}_3$, …, $\mathbf{r}_n$ has a point vector $\bar{\mathbf{r}}$ defined as

$$\bar{\mathbf{r}} = \frac{\sum_{i=1}^{n} \mathbf{r}_i \Delta_i}{\sum_{i=1}^{n} \Delta_i}$$

where $\Delta_i$ is the $i$ th quantity (for example, this could be the length, area, volume, or mass of an element), $\mathbf{r}_i$ is the position vector of $i$ th element, $\sum_{i=1}^{n} \Delta_i$ is the sum of all $n$ elements, and $\sum_{i=1}^{n} \mathbf{r}_i \Delta_i$ is the first moment of all elements relative to the selected point O. In terms of x, y, and z coordinates, the centroid has coordinates

$$\bar{x} = \frac{\sum_{i=1}^{n} x_i \Delta_i}{\sum_{i=1}^{n} \Delta_i}, \quad \bar{y} = \frac{\sum_{i=1}^{n} y_i \Delta_i}{\sum_{i=1}^{n} \Delta_i}, \quad \bar{z} = \frac{\sum_{i=1}^{n} z_i \Delta_i}{\sum_{i=1}^{n} \Delta_i}$$

where $\Delta_i$ is the magnitude of the $i$ th quantity (element), $\bar{x}$, $\bar{y}$, $\bar{z}$ are the coordinates of centroid of the assemblage, and $x_i$, $y_i$, $z_i$ are the coordinates of $P_i$ at which $\Delta_i$ is concentrated.

The centroid of a continuous quantity may be located though calculus by using infinitesimal elements of the quantity. Thus, for area A and in terms of x, y, z coordinates, we can write

$$\begin{cases} \bar{x} = \dfrac{\int x dA}{\int dA} = \dfrac{Q_{yz}}{A} \\ \bar{y} = \dfrac{\int y dA}{\int dA} = \dfrac{Q_{xz}}{A} \\ \bar{z} = \dfrac{\int z dA}{\int dA} = \dfrac{Q_{xy}}{A} \end{cases}$$

where $Q_{xy}$ , $Q_{yz}$ , $Q_{xz}$ are first moments with respect to the xy, yz, and xz planes, respectively. The following table indicates the first moments $Q$ of various quantities $\Delta$ about the coordinate planes. In Table 3-1 $Q_{xy}$ , $Q_{yz}$ , $Q_{xz}$ are the first moments with respect to xy, yz, xz planes, $L$ is the length, and $m$ is the mass, respectively. Note that in two-dimensional work, e.q. in the xy plane, $Q_{xy}$ becomes $Q_x$, and $Q_{yz}$ becomes $Q_y$ .

Table 3-1. First moment $Q$ of various quantities.

| $\Delta$ | $Q_{xy}$ | $Q_{yz}$ | $Q_{xz}$ | Dimensions |
|---|---|---|---|---|
| Line | $\int zdL$ | $\int xdL$ | $\int ydL$ | $L^2$ |
| Area | $\int zdA$ | $\int xdA$ | $\int ydA$ | $L^3$ |
| Volume | $\int zdV$ | $\int xdV$ | $\int ydV$ | $L^4$ |
| Mass | $\int zdm$ | $\int xdm$ | $\int ydm$ | $mL$ |

Now let us consider the case illustrated in Fig.3-2, which is a cross section of the finger. According to the figure, $\bar{y}$ can be expressed as

$$\bar{y} = R = \frac{\int ydA}{\int dA} = \frac{Q_x}{A}$$

If we choose the polar coordinate system y is represented by,

$$y = r\cos\theta$$

Using this polar coordinate system, the $\bar{y}$ of the centroid can be calculated by,

$$\bar{y} = \frac{Q_x}{A} = \frac{\int ydA}{\int dA} = \frac{\int_\alpha^\beta \int_{R_1}^{R_2} r\cos(\theta) r dr d\theta}{\int_\alpha^\beta \int_{R_1}^{R_2} r dr d\theta}$$

$$= \frac{\left[\frac{1}{3}r^3\right]_{R_1}^{R_2} \int_\alpha^\beta \cos(\theta) d\theta}{\left[\frac{1}{2}r^2\right]_{R_1}^{R_2} \int_\alpha^\beta d\theta}$$

$$= \frac{2\left(R_2{}^3 - R_1{}^3\right)}{3\left(R_2{}^2 - R_1{}^2\right)} \frac{\sin(\beta) + \sin(\alpha)}{\beta - \alpha}$$

$$= \frac{2\left(R_2{}^3 - R_1{}^3\right)}{3\left(R_2{}^2 - R_1{}^2\right)} \frac{\sin(\beta) + \sin(\alpha)}{\beta - \alpha}$$

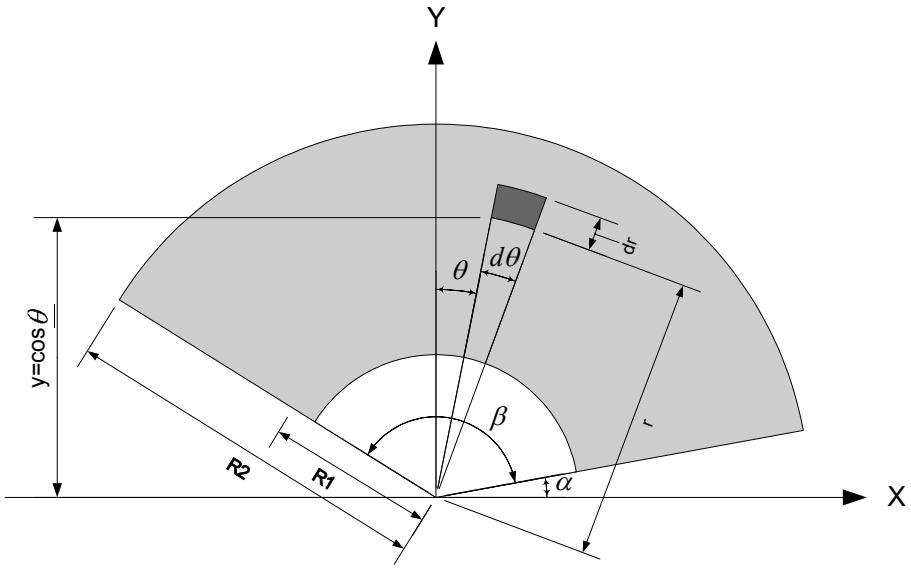


Figure 3-2. Cross sectional area of the finger.

If $\alpha = 0$,

$$\overline{x} = \frac{2\left(R_2{}^3 - R_1{}^3\right)}{3\left(R_2{}^2 - R_1{}^2\right)} \frac{\sin(\beta)}{\beta}$$

Since the centroid of the cross section is always located along the symmetric line of the finger, it is convenient if the y-axis is chosen such that the centroid is located on the y-axis, as illustrated in Fig.3-3. Due to the symmetry, the integration of the domain can be done between $-\alpha$ and $\alpha$ for angles, which provides a convenient formula. If we choose the polar coordinate system, from the Fig.3-3, y is represented by,

$$y = r\cos\theta$$

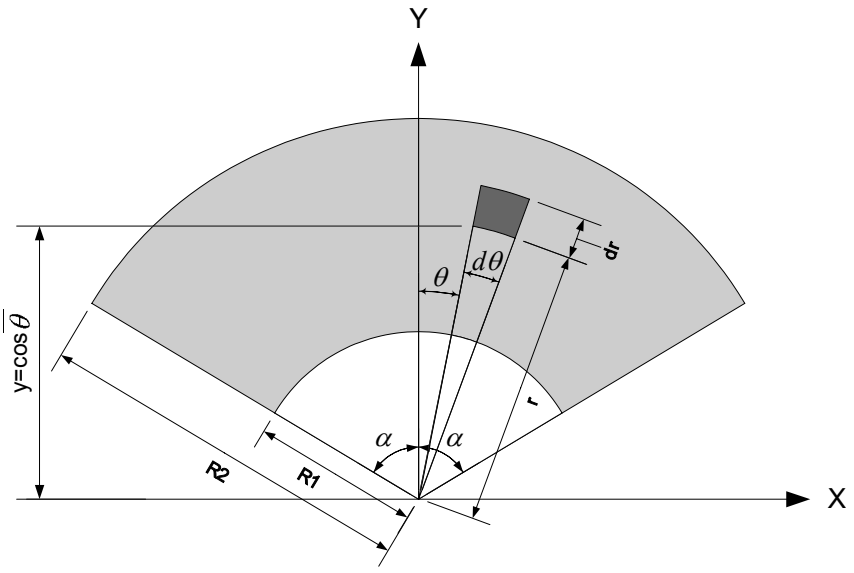


Figure 3-3. Cross sectional area of the finger.

Using this polar coordinate system, the $\bar{y}$ of the centroid can be calculated by,

$$\bar{y} = R = \frac{Q_x}{L} = \frac{\int y dA}{\int dA} = \frac{\int_{-\alpha}^{\alpha}\int_{R_1}^{R_2} r\cos(\theta) r dr d\theta}{\int_{-\alpha}^{\alpha}\int_{R_1}^{R_2} r dr d\theta}$$

$$= \frac{\left[\frac{1}{3}r^3\right]_{R_1}^{R_2}\int_{-\alpha}^{\alpha}\cos(\theta)d\theta}{\left[\frac{1}{2}r^2\right]_{R_1}^{R_2}\int_{-\alpha}^{\alpha}d\theta}$$

$$= \frac{2\left(R_2{}^3 - R_1{}^3\right)}{3\left(R_2{}^2 - R_1{}^2\right)}\frac{\sin(\alpha)-\sin(-\alpha)}{\alpha-(-\alpha)}$$

$$= \frac{2\left(R_2{}^3 - R_1{}^3\right)}{3\left(R_2{}^2 - R_1{}^2\right)}\frac{\sin(\alpha)}{\alpha}$$

$$\therefore R = \frac{2\left(R_2{}^3 - R_1{}^3\right)}{3\left(R_2{}^2 - R_1{}^2\right)}\frac{\sin(\alpha)}{\alpha} \tag{3.3}$$

This equation can be used for the general case which undergoes the centrifugal force. For the simplified model in Chapter 2, $\alpha = \frac{\pi}{2}$, $R_2 = 4.7625mm$, $R_1 = 1.5mm$.

Substituting these values into the above equation yields $\bar{y} = R = 2.1738mm$. Substituting this value into Eq.(3.2) yields the normal force and the contact pressure between two contact surfaces. In Eq.(3.2), the contact area $A_c$ can be calculated by

$$A_c = \pi R_2 L = \pi \times 4.7625 \times 101.6 = 1520 \quad [mm^2]$$

which assumes that all parts of the surface are in contact. Using the material properties shown in Table 2-1, the mass $M$ can be calculated by.

$$M = \rho V = 7.82 \times 10^{-6} \times \frac{\pi}{2}\left(4.7625^2 - 1.5^2\right) \times 101.6$$
$$= 2.5499 \times 10^{-2} \quad [kg]$$

Therefore the contact pressure can be obtained from Eq.(3.2), as

$$\therefore P_c = \frac{MR\omega^2}{A_c} = \frac{2.5499 \times 10^{-2} \times 2.1738 \times 2722.713^2}{1520}$$
$$= 270.33 \quad [KPa] = 0.2703 \quad [MPa]$$

It is noted that the contact pressure $P_c$ is calculated from the assumption that the whole surface is in contact with a constant pressure.

**Calculation of the Relative Displacement and the Work**

In this section the relative displacement that is caused by the vertical force (cutting force) will be calculated and the work that has been done by the friction force will be calculated. This state represents the one in which the endmill starts the cutting operation. The same assumptions are used as in the last case except for the second one because there is now a relative motion between the two contact surfaces. The assumptions are:

- There is no angular acceleration, which means the angular velocity is constant.
- There is no normal contact force change caused by the vertical force.
- Contact occurs throughout the entire contact area.

Because the centrifugal force is dominant in this endmill system, the change of the normal contact force due to the vertical force is ignored in this step. The first step of calculating the frictional work is to obtain the second moment of inertia of the finger. The following definitions of the second moment, or moment of inertia are analogous to the definitions of the first moment of a plane area, which were given in the previous section. The derivation of load-stress formulas for beams may require solutions of one or more of the following equations:

$$\begin{cases} I_x = \int y^2 dA \\ I_y = \int x^2 dA \\ I_{xy} = \int xy dA \end{cases} \tag{3.4}$$

where $dA$ is an element of the plane area $A$ lying in the x-y plane. $A$ represents the cross-sectional area of a member subjected to bending and/or torsional loads. The integrals in the above equations are commonly called moments of inertia of the area $A$ because of the similarity with integrals that define the moment of inertia of bodies in the field of dynamics. From Eq.(3.4), if we choose the polar coordinate system, x and y are represented as,

$$x = r\cos\theta, \qquad y = r\sin\theta$$

and $I_x$, $I_y$, $I_{xy}$ are

$$\begin{cases} I_x = \int_\alpha^\beta \int_{R_1}^{R_2} r^3 \sin^2\theta dr d\theta = \frac{1}{8}\left(R_2{}^4 - R_1{}^4\right)\left(\beta - \alpha - \sin\beta\cos\beta + \sin\alpha\cos\alpha\right) \\ I_y = \int_\alpha^\beta \int_{R_1}^{R_2} r^3 \cos^2\theta dr d\theta = \frac{1}{8}\left(R_2{}^4 - R_1{}^4\right)\left(\beta - \alpha + \sin\beta\cos\beta - \sin\alpha\cos\alpha\right) \\ I_{xy} = \int_\alpha^\beta \int_{R_1}^{R_2} r^3 \sin\theta\cos\theta dr d\theta = \frac{1}{8}\left(R_2{}^4 - R_1{}^4\right)\left(\sin^2\beta - \sin^2\alpha\right) \end{cases} \tag{3.5}$$

If $\alpha = 0$ the Eq.(3.5) can be written as

$$\begin{cases} I_x = \int_0^{\alpha}\int_{R_1}^{R_2} r^3 \sin^2\theta dr d\theta = \frac{1}{8}\left(R_2{}^4 - R_1{}^4\right)\left(\alpha - \sin\alpha\cos\alpha\right) \\ I_y = \int_0^{\alpha}\int_{R_1}^{R_2} r^3 \cos^2\theta dr d\theta = \frac{1}{8}\left(R_2{}^4 - R_1{}^4\right)\left(\alpha + \sin\alpha\cos\alpha\right) \\ I_{xy} = \int_0^{\alpha}\int_{R_1}^{R_2} r^3 \sin\theta\cos\theta dr d\theta = \frac{1}{8}\left(R_2{}^4 - R_1{}^4\right)\sin^2\alpha \end{cases} \tag{3.6}$$

For the simplified model in Chapter 2, $\alpha = \pi$, $R_1 = 1.5mm$, $R_2 = 4.7625mm$. Substituting those values into the above equation yields,

$$I_x = \frac{1}{8}\left(4.7625^4 - 1.5^4\right)\left(\pi - \sin\pi\cos\pi\right) = \frac{\pi}{8}\left(4.7625^4 - 1.5^4\right)$$

Thus, the moment of inertia of the upper finger is

$$I_x = \frac{\pi}{8}\left(R_3{}^4 - R_4{}^4\right) = \frac{\pi}{8}\left(4.7625^4 - 1.5^4\right) = 200 \quad [mm^4]$$

The moment of inertia of the lower finger can be obtained in the same way because the two fingers are symmetric about the x-axis, and the two values would be the same.

Now let us calculate the relative displacement and the friction work. It is well known that beams undergo internal shear deformations along their axes during bending. Members of a composite beam that are not securely fixed together will slide over each other in proportion to their distance from the neutral axis of entire composite beam. It is known that for a cantilevered beam with a point load at the end, the vertical deflection at any point in the beam's neutral surface is

$$\delta = \frac{F}{6EI}\left(-x^3 + 3xL^2 - 2L^3\right)$$

where *F* is the force on the end of the beam, *E* is the beam's elastic modulus, *I* is the beam's moment of inertia, *x* is the position along the length of the beam measured from the free end, and *L* is the length of the beam.

If a composite beam is bent, all members will have the same deflection at the tip. Therefore it can be written that

$$\delta = \frac{F_s}{6E_sI_s}\left(-x^3 + 3xL^2 - 2L^3\right) = \frac{F_f}{6E_fI_f}\left(-x^3 + 3xL^2 - 2L^3\right) \tag{3.7}$$

where, subscript *s* means the shank, and *f* means the finger. The external force *F* at the tip of the endmill must equal the sum of the forces required to deflect each member.

$$F = F_s + \sum F_f \tag{3.8}$$

If there are only two fingers inside the shank Eq.(3.7) can be written as

$$\frac{F_s}{E_sI_s} = \frac{F_{f1}}{E_{f1}I_{f1}} = \frac{F_{f2}}{E_{f2}I_{f2}}$$

The above equation can be written as follows

$$F_s = \frac{F_{f1}E_sI_s}{E_{f1}I_{f1}}, \text{ and } F_{f2} = \frac{F_{f1}E_{f2}I_{f2}}{E_{f1}I_{f1}}$$

Substituting these equations into (3.8) yields

$$F = F_s + F_{f1} + F_{f2} = \frac{F_{f1}E_sI_s}{E_{f1}I_{f1}} + F_{f1} + \frac{F_{f1}E_{f2}I_{f2}}{E_{f1}I_{f1}}$$

Solving above equation for $F_{f1}$ yields

$$F_{f1} = \frac{FE_{f1}I_{f1}}{\left(E_sI_s + E_{f1}I_{f1} + E_{f2}I_{f2}\right)}$$

This equation can be reduced to

$$F_{f1} = \frac{FE_{f1}I_{f1}}{E_sI_s + \sum_{i=1}^{n} E_{fi}I_{fi}}$$

The same operation for $F_s$ and $F_{f2}$ yields

$$F_s = \frac{FE_sI_s}{E_sI_s + \sum_{i=1}^{n} E_{fi}I_{fi}}$$

$$F_{f2} = \frac{FE_{f2}I_{f2}}{E_sI_s + \sum_{i=1}^{n} E_{fi}I_{fi}}$$

The normal stress at any point in a cantilevered beam is given by

$$\sigma = \frac{Fxc}{I}$$

where $\sigma$ is the stress, $F$ is the force on the free end, $x$ is the position along the beam measured from the free end, $c$ is the distance from the beam's neutral axis to the point of interest, and $I$ is the area moment of inertia of its cross section. The axial strain in the beam is then

$$\varepsilon = \frac{\sigma}{E} = \frac{Fxc}{EI}$$

where $\varepsilon$ is the axial strain and $E$ is the Young's Modulus of the material. $c$ is the sum of the quantity $(d+y)$ where $d$ is the distance of the neutral axis of the finger from the neutral axis of the composite beam and $y$ is the perpendicular distance from the point in question to the neutral axis of the finger.

For any point in any component member of the composite beam, the change in position of the point related to $x$=0 (the free end of the beam) can be written as

$$\delta_{axial} = \int_0^x \varepsilon dx$$

Substituting the previously obtained equations into this integral for both the fingers and the shank, the following equations are obtained. The value of $d$ of the finger can be

represented by $R \times \sin\theta$, where $\theta$ is the start angle. Note that in the equation for the shank, *d* is zero because its neutral axis lies on the neutral axis of the composite beam.

$$\delta_{saxial} = \int_x^L \frac{F \times x \times (d+y)}{EI} dx = \frac{FE_s I_s}{E_s I_s + \sum_{i=1}^{n} E_{fi} I_{fi}} \frac{(0+y)}{2E_s I_s} (L^2 - x^2) = \frac{F \times y \times (L^2 - x^2)}{2\left( E_s I_s + \sum_{i=1}^{n} E_{fi} I_{fi} \right)}$$

$$\delta_{faxial} = \int_x^L \frac{F \times x \times (d+y)}{EI} dx = \frac{FE_{fi} I_{fi}}{E_s I_s + \sum_{i=1}^{n} E_{fi} I_{fi}} \frac{(d+y)}{2E_{fi} I_{fi}} (L^2 - x^2) = \frac{F \times (d+y) \times (L^2 - x^2)}{2\left( E_s I_s + \sum_{i=1}^{n} E_{fi} I_{fi} \right)}$$

The relative displacement can then be obtained by subtracting the above two equations

$$\delta_{faxial} - \delta_{saxial} = \frac{F \times (d+y) \times (L^2 - x^2)}{2\left( E_s I_s + \sum_{i=1}^{n} E_{fi} I_{fi} \right)} - \frac{F \times y \times (L^2 - x^2)}{2\left( E_s I_s + \sum_{i=1}^{n} E_{fi} I_{fi} \right)} = \frac{F \times d \times (L^2 - x^2)}{2\left( E_s I_s + \sum_{i=1}^{n} E_{fi} I_{fi} \right)}$$

The work done through this displacement is by friction. The amount of work done is equal to the integral solved over the entire length of the beam of the frictional force (friction coefficient times the normal force, which is the force/unit length at a point times the differential length) multiplied by the relative displacement. Writing this equation (assuming the pressure, *P*, is uniform over the entire area of the finger)

$$\mu P(\delta_{f_{axial}} - \delta_{saxial}) = \int_0^L \mu P \frac{F \times d \times (L^2 - x^2)}{2\left( E_s I_s + \sum_{i=1}^{n} E_{fi} I_{fi} \right)} dx$$

The work done by friction for a displacement of the end of the beam by a specified force, *F*, is then

$$W = \frac{1}{3} L^3 \mu PF \frac{d}{\left( E_s I_s + \sum_{i=1}^{n} E_{fi} I_{fi} \right)} \tag{3.9}$$

The MATLAB code used for calculating this friction work is implemented in appendix A. Figure 3-4, 3-5 and 3-6 show the results of theoretical analysis.

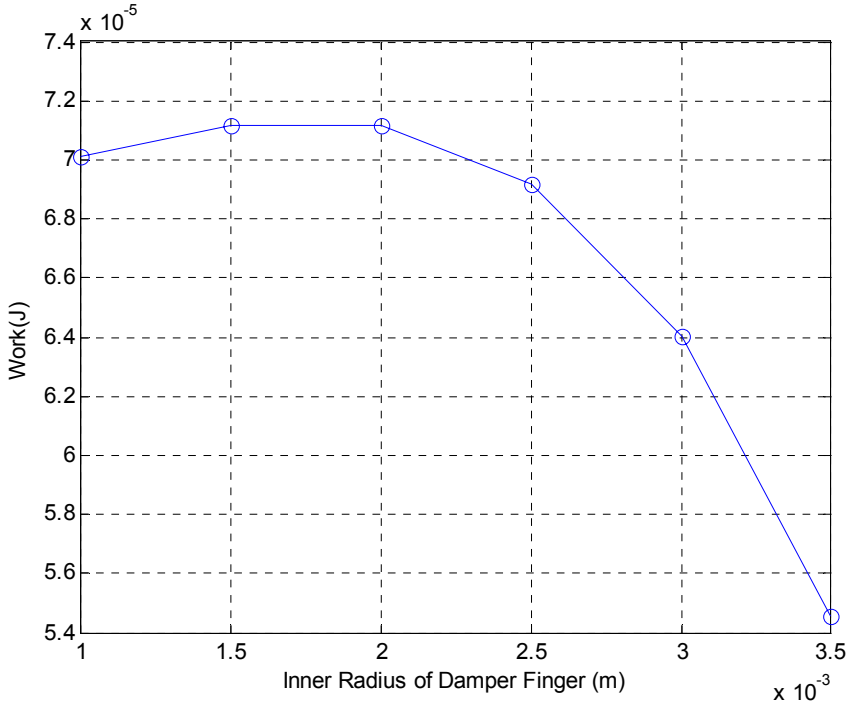


Figure 3-4. Plot of work done by the friction force according to the change of the inner radius of finger.

Figure 3-4 is the work according to the change of the inner radius of the finger. As the radius increases the work decreases because the mass decreases. When the radius is 1.5mm and the number of finger is 2, the work done by the friction force is $7.1182\times10^{-5}[J]$. Figure 3-5 is the work calculated for different values of the start angle when the number of damper fingers is two and the inner radius is 1.5 mm. When the start angle is 0 it has its maximum value and this value gradually decreases as the angles decrease. Even when the number of fingers is held constant, the damping values differ for different positions of the finger. This result is reasonable because the relative displacement is zero at the neutral axis. In Chapter 6 this effect will be discussed in more detail.

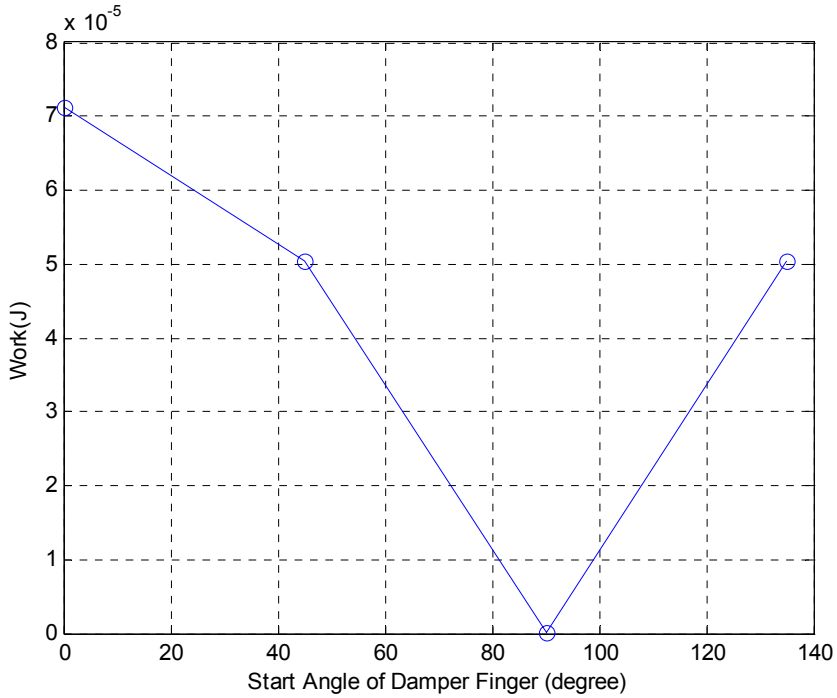


Figure 3-5. Plot of work done by the friction force for varying start angles of the finger. The radius of the finger is 1.5 mm and the number of the finger is 2.

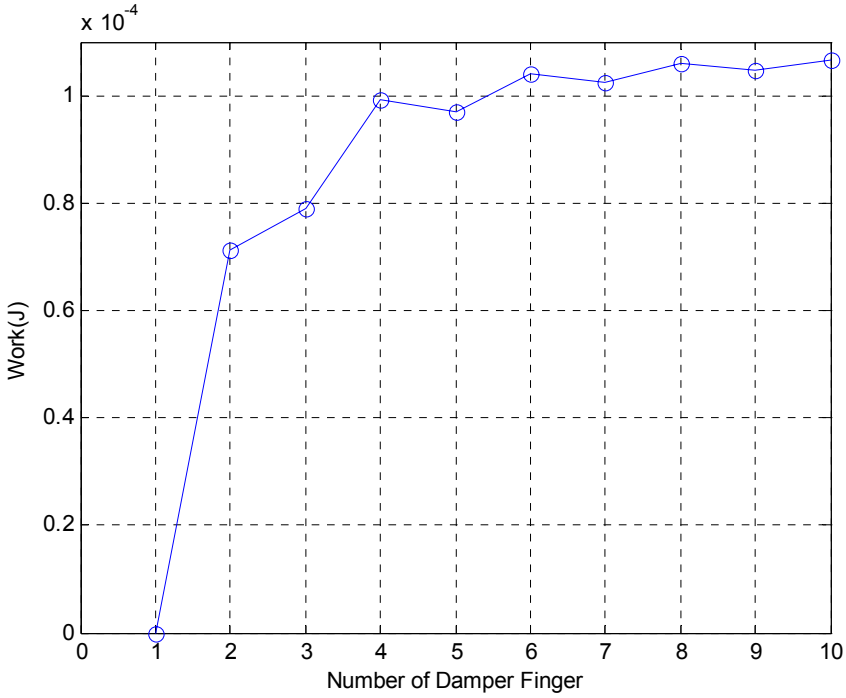


Figure 3-6. Plot of the work done by the friction force for different numbers of damper fingers. The inner radius of the finger is 1.5 mm and the start angle is chosen to have the maximum damping in each number of the finger.

Figure 3-6 shows the work for different numbers of fingers. The inner radius of the finger is 1.5 mm and the start angle is chosen to have the maximum damping for the number of fingers being used. The work increases gradually as the number of fingers is increased. Finite element analysis will be done for these analytical results in the following chapter.

# CHAPTER 4
# BACKGROUND OF FINITE ELEMENTANALYSIS IN CONTACT PROBLEMS

Since the material properties of the endmill is linear elastic, the classical finite element can be used without difficulty. Major concern is the contact constraints in the interface. Contact problems are highly nonlinear and require significant computer resources to solve for. Contact problems present two significant difficulties. First, the regions of contact are generally unknown until running the model. Depending on the loads, material, boundary conditions, and other factors, surfaces can come into and go out of contact with each other in a largely unpredictable and abrupt manner. Second, most contact problems need to account for friction. Frictional response can be chaotic, making solution convergence difficult. In addition to these two difficulties, many contact problems must also address multi-field effects, such as the conductance of heat and electrical currents in the areas of contact. In this chapter the general procedure of performing the contact analysis using FEA is discussed.

Contact problems are characterized by contact constraints which must be imposed on contacting boundaries. To impose the contact constraints, two basic methods are available: the Lagrange multiplier method [9] and the penalty method [9]. Other constraint methods based on the basic methods have been proposed and applied. The augmented Lagrangian method [9] and the perturbed Lagrangian method [9] are two examples.

## Contact Formulation in Static Problems

To introduce the basic constraint methods, we consider static mechanical problems subjected to contact constrains on known contacting boundaries. For small displacements, the total potential energy of the structure can be written as,

$$\Pi(\mathbf{u}) = \frac{1}{2}\int_{\Omega} \mathbf{e}^T \mathbf{C}\mathbf{e} d\Omega - \int_{\Omega} \mathbf{u}\cdot\mathbf{b} d\Omega - \int_{\Omega} \mathbf{u}\cdot\mathbf{q} dS - \mathbf{U}_d^T \mathbf{F} \tag{4.1}$$

where $\Pi$ is the total potential energy of the body, $e$ is the engineering strain, $C$ is the elastic modulus, $b$ is the body force, $q$ is the surface traction. By using standard element procedures, the discretized form of Eq.(4.1) can be obtained as follows:

$$\Pi(\mathbf{U}) = \frac{1}{2}\mathbf{U}^T\mathbf{K}\mathbf{U} - \mathbf{U}^T\mathbf{F} \tag{4.2}$$

where $U$ is the global displacement vector, $K$ is the global stiffness matrix, and $F$ is the global load vector.

The virtual work due to the contact load is calculated as

$$\delta W_c = \sum_{n=1}^{{}^tL} (\delta w_c)^n \tag{4.3}$$

where $(\ )^n$ indicates that the quantity in the parentheses is evaluated in association with a hitting node n, ${}^tL$ is the total number of hitting nodes at time t, and $\delta w_c$ the virtual work due to the concentrated contact force at hitting node $n$ and is calculated as

$$\delta w_c = {}^t f_i (\delta \mathbf{u}^2 - \delta \mathbf{u}^1) \cdot {}^t\mathbf{N}_i \tag{4.4}$$

where ${}^t f_i$ is the components of the contact force at a target point in the directions of ${}^t\mathbf{N}_i$. The virtual displacement $\delta\mathbf{u}^2$ at the target point can be evaluated by using equation

$$\delta \mathbf{u}^2 = \sum_{n=1}^{N} \phi_n \delta \mathbf{u}^{2,n} \tag{4.5}$$

where $N$ denotes the total number of target nodes on the target segment, $\phi_n$ denotes the shape function associated with contact node $n$ on the contact segment and $\delta\mathbf{u}^{2,n}$ is the displacement of target node $n$.

To obtain a matrix expression for $\delta\mathbf{u}^2 - \delta\mathbf{u}^1$, the following notation is used:

$$\mathbf{u}_c = \left\{ u_1^1 \quad u_2^1 \quad u_3^1 \quad u_1^{2,1} \quad u_2^{2,1} \quad u_3^{2,1} \quad \ldots \quad u_1^{2,N} \quad u_2^{2,N} \quad u_3^{2,N} \right\}^T$$

$$\mathbf{Q}_c = \begin{bmatrix} -1 & 0 & 0 & \phi_1 & 0 & 0 & \phi_2 & 0 & 0 & 0 & \phi_N & 0 & 0 \\ 0 & -1 & 0 & 0 & \phi_1 & 0 & 0 & \phi_2 & 0 & \ldots & 0 & \phi_N & 0 \\ 0 & 0 & -1 & 0 & 0 & \phi_1 & 0 & 0 & \phi_2 & 0 & 0 & 0 & \phi_N \end{bmatrix}$$

Then Eq.(4.4) can be written as

$$\delta w_c = \delta\mathbf{u}_c^T \left( \mathbf{Q}_c^T \, {}^t\mathbf{N}_i \, {}^t f_i \right) = \delta\mathbf{u}_c^T \, {}^t\mathbf{r}_c$$

where

$${}^t\mathbf{N}_i = \left\{ {}^tN_{i1} \quad {}^tN_{i2} \quad {}^tN_{i3} \right\}^T$$

$${}^t\mathbf{r}_c = \mathbf{Q}_c^T \, {}^t\mathbf{N}_i \, {}^t f$$

where ${}^tN_{ij}$ denotes the $j$ th component of the boundary unit vector ${}^t\mathbf{N}_i$.

We realize that ${}^t\mathbf{r}_c$ is a nodal force vector contributed by the contact at the associated contacting node. It will be convenient to distinguish, in the evaluation of ${}^t\mathbf{r}_c$, between the contribution of normal contact forces and the contribution of tangential friction forces. Thus we write

$${}^t\mathbf{r}_c = {}^t\mathbf{r}_{cn} + {}^t\mathbf{r}_{cf}$$

where

$${}^t\mathbf{r}_{cn} = \mathbf{Q}_c^T \, {}^t\mathbf{N}_1 \, {}^t f_1$$

$${}^t\mathbf{r}_{cf} = \mathbf{Q}_c^T \, {}^t\mathbf{N}_J \, {}^t f_J \qquad \textit{summation on } J = 2,3$$

The penetration of the hitting node can be calculated as

$$ {}^{t}p = \left( {}^{t}\mathbf{x}^{2} - {}^{t}\mathbf{x}^{1} \right) \cdot {}^{t}\mathbf{N}_{1} $$

where ${}^{t}\mathbf{x}^{1}$ and ${}^{t}\mathbf{x}^{2}$ are the position vectors of the hitting node and target point, respectively.

Expressing ${}^{t}\mathbf{x}^{1}$ and ${}^{t}\mathbf{x}^{2}$ in terms of the displacements $\mathbf{u}^{1}$ and $\mathbf{u}^{2}$, respectively, we have the following discrete form of the kinematic contact condition:

$$ \begin{aligned} {}^{t}p &= \left( {}^{t}\mathbf{x}^{2} - {}^{t}\mathbf{x}^{1} \right) \cdot {}^{t}\mathbf{N}_{1} + \left( \mathbf{u}^{2} - \mathbf{u}^{1} \right) \cdot {}^{t}\mathbf{N}_{1} \\ &= {}^{t}\tilde{\mathbf{N}}_{1}^{T}\mathbf{Q}_{c}\mathbf{u}_{c} + {}^{\tau}p = 0 \end{aligned} \tag{4.6} $$

where

$$ {}^{\tau}p = {}^{t}\tilde{\mathbf{N}}_{1}^{T}{}^{\tau}\overline{\mathbf{X}} $$

$$ {}^{\tau}\overline{\mathbf{X}} = \left\{ {}^{\tau}x_{1}^{2} - {}^{\tau}x_{1}^{1},\ {}^{\tau}x_{2}^{2} - {}^{\tau}x_{2}^{1},\ {}^{\tau}x_{3}^{2} - {}^{\tau}x_{3}^{1} \right\}^{T} $$

This means that for small displacements the configuration of the contact system may be considered unchanged after the displacements. Thus, we can approximate ${}^{t}\tilde{\mathbf{N}}_{1}$, by ${}^{0}\tilde{\mathbf{N}}_{1}$ in Eq.(4.6). Furthermore, we assume only one load step. This means that we need to move only one step in the "time" domain and ${}^{\tau}p$ and ${}^{t}p$ in Eq.(4.6) can be replaced by ${}^{0}p$ and $p$, respectively, where ${}^{0}p$ denotes any initial penetration (or gap) and $p$ any penetration after deformation. Therefore, the discretized kinematic contact condition can now be written as

$$ p = {}^{o}\tilde{\mathbf{N}}_{1}^{T}\mathbf{Q}_{c}\mathbf{u}_{c} + {}^{0}p = 0 \tag{4.7} $$

Eq.(4.7) applies to a single contacting node. If there are $L (L > 1)$ contacting nodes, there will be $L$ contact constraint equations, each taking the form of Eq.(4.7). Those $L$ contact constraint equations can be assembled to obtain

$$\mathbf{P} = \mathbf{QU} + {}^{0}\mathbf{P} = 0 \tag{4.8}$$

where

$$\mathbf{P} = \{p^1, p^2, ..., p^L\}^T$$

$$\mathbf{Q} = \sum_{I=1}^{L} \left[ {}^{0}\mathbf{N}_1^T \mathbf{Q}_c \right]_I$$

$${}^{0}\mathbf{p} = \left\{ {}^{0}p^1, \ {}^{0}p^2, ..., {}^{0}p^L \right\}^T$$

Since the contacting boundaries are known, all the contacting nodes can be identified and Eq.(4.8) can be established explicitly.

Based on the above preparations, the contact problem can be stated as follows:

Minimize $\Pi(\mathbf{U})$ in Eq.(4.2) subject to the constraints in Eq.(4.8) [P-1]

It must be observed that the mechanical contact condition should be satisfied automatically by assuming that all the $L$ contact nodes are actual contacting nodes. In general, actual contacting nodes are not known a priori and an iterative trial-and-error procedure is required to find all contacting nodes. In the following, we discuss the solution of problem [P-1] with alternative constraint methods.

**The Lagrange Multiplier Method**

In the Lagrange multiplier method, the function to be minimized is replaced by the following function:

$$\prod_L (\mathbf{U}, \mathbf{\Lambda}) = \frac{1}{2}\mathbf{U}^T\mathbf{KU} - \mathbf{U}^T\mathbf{F} + \mathbf{\Lambda}^T(\mathbf{QU} + {}^{0}\mathbf{P}) \tag{4.9}$$

where $\mathbf{\Lambda}$ is an unknown vector which contains as many elements as there are constraint equations in Eq.(4.8). The elements in $\mathbf{\Lambda}$ are known as Lagrange multipliers.

The constrained minimization problem [P-1] is now transformed into the following saddle-point problem:

Find $\mathbf{U}$ and $\mathbf{\Lambda}$ such that $\prod_L(\mathbf{U},\mathbf{\Lambda})$ is stationary, i.e. [P-2]

$$\begin{aligned}\frac{\partial \prod_L}{\partial \mathbf{U}} &= 0\\ \frac{\partial \prod_L}{\partial \mathbf{\Lambda}} &= 0\end{aligned} \tag{4.10}$$

Eq.(4.10) yields

$$\begin{aligned}\mathbf{KU} - \mathbf{F} + \mathbf{QH}^T\mathbf{\Lambda} &= 0\\ \mathbf{QU} +^0 \mathbf{P} &= 0\end{aligned} \tag{4.11}$$

Combining Eq.(4.11), we obtain

$$\mathbf{K}_L\mathbf{U}_L = \mathbf{F}_L \tag{4.12}$$

where

$$\mathbf{K}_L = \begin{bmatrix}\mathbf{K} & \mathbf{Q}^T\\ \mathbf{Q} & 0\end{bmatrix}$$

$$\mathbf{F}_L = \begin{Bmatrix}\mathbf{U}\\ -^0\mathbf{P}\end{Bmatrix}$$

$$\mathbf{U}_L = \begin{Bmatrix}\mathbf{U}\\ \mathbf{\Lambda}\end{Bmatrix}$$

By solving Eq.(4.12), we can obtain the displacement $\mathbf{U}$ and the Lagrange multiplier $\mathbf{\Lambda}$. The elements in $\mathbf{\Lambda}$ are interpreted as contacting forces at the corresponding contacting nodes.

**The Penalty Method**

In the penalty method, the potential energy of the structure is penalized when a penetration occurs on the contact surface. The following penalty potential is added to the structural potential:

$$\pi_p = \frac{1}{2}\mathbf{P}^T \alpha \mathbf{P}$$

where $\boldsymbol{\alpha}$ is a diagonal matrix with elements $\alpha_{ii}$, which is the penalty parameters and $\mathbf{P}$ is a vector of penetration..

The function to be minimized is now replaced by

$$\begin{aligned} \Pi_p &= \Pi + \pi_p \\ &= \frac{1}{2}\mathbf{U}^T\mathbf{K}\mathbf{U} - \mathbf{U}^T\mathbf{F} + \frac{1}{2}\mathbf{P}^2\boldsymbol{\alpha}\mathbf{P} \end{aligned} \tag{4.13}$$

The constrained minimization problem [P-1] is then transformed into the following unconstrained minimization problem:

Find $\mathbf{U}$ such that $\Pi_p$ is minimized.

To find its minimum, $\Pi_L$ is held stationary by invoking the following condition:

$$\frac{\partial \Pi_p}{\partial \mathbf{U}} = 0 \tag{4.14}$$

Substituting Eq.(4.13) and (4.8) into (4.14), we can obtain

$$\mathbf{K}_p\mathbf{U} = \mathbf{F}_p \tag{4.15}$$

where

$$\mathbf{K}_p = \mathbf{K} + \mathbf{Q}^T\boldsymbol{\alpha}\mathbf{Q}$$
$$\mathbf{F}_P = \mathbf{F} - \mathbf{Q}^T\boldsymbol{\alpha}^0\mathbf{P}$$

The solution of Eq.(4.15) gives the displacement $\mathbf{U}$. The contacting forces are then calculated as

$$\mathbf{F}_C = \boldsymbol{\alpha}\mathbf{P}$$

where the penetration $\mathbf{P}$ is a function of the displacement vector $\mathbf{U}$.

CHAPTER 5
FIITE ELEMENT ANALYSIS

In this chapter, the finite element analysis procedure and results of the endmill system are presented. Even though the cutting process is dynamic, a static finite element analysis is performed with the centrifugal force and the cutting force at the tip. Thus, the friction work obtained must be interpreted as a qualitative measure. Since the simulation condition is the same as that of the analytical method in Chapter 3, it is still valid to compare the results of finite element analysis with the analytical results.

**Finite Element Model**

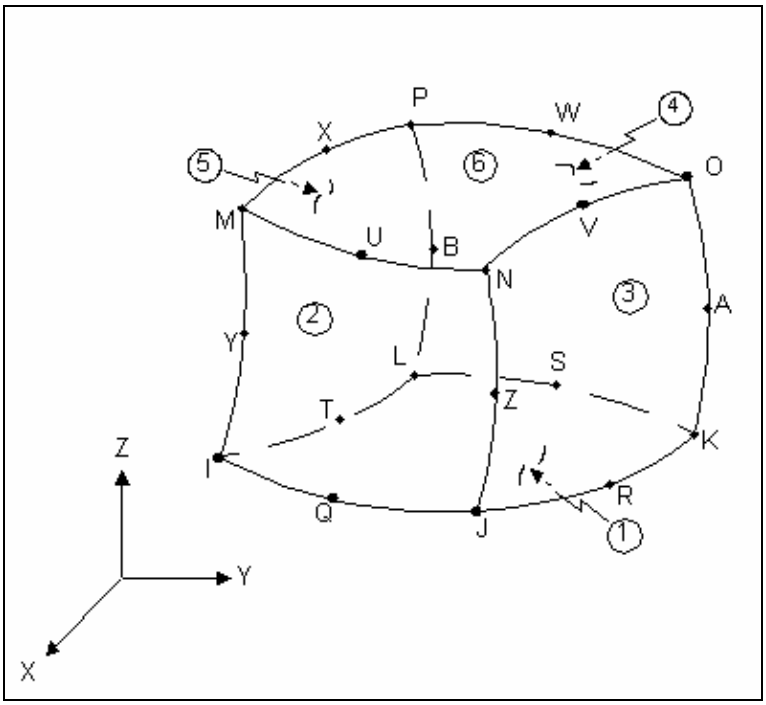


Figure 5-1. Solid 95, 20 node solid element

The first step of finite element analysis is to build a computational model. The simplified geometry for the endmill in Chapter 2 is used in the FEA. Using the same

material properties listed in Table 2-1, 20-node solid elements in ANSYS (solid 95) are used to build the shank and finger. Figure 5-1 illustrates a 20-node solid element that is used in ANSYS, and Fig.5-2 plots the finite element model of the endmill with boundary conditions. In Fig.5-2, the shank is modeled using two elements through the radial direction, and fingers are modeled inside the shank. The cutting force F=100N is distributed to 4 nodes at the tip. Table5-1 shows the number of elements used in the endmill finite element model.

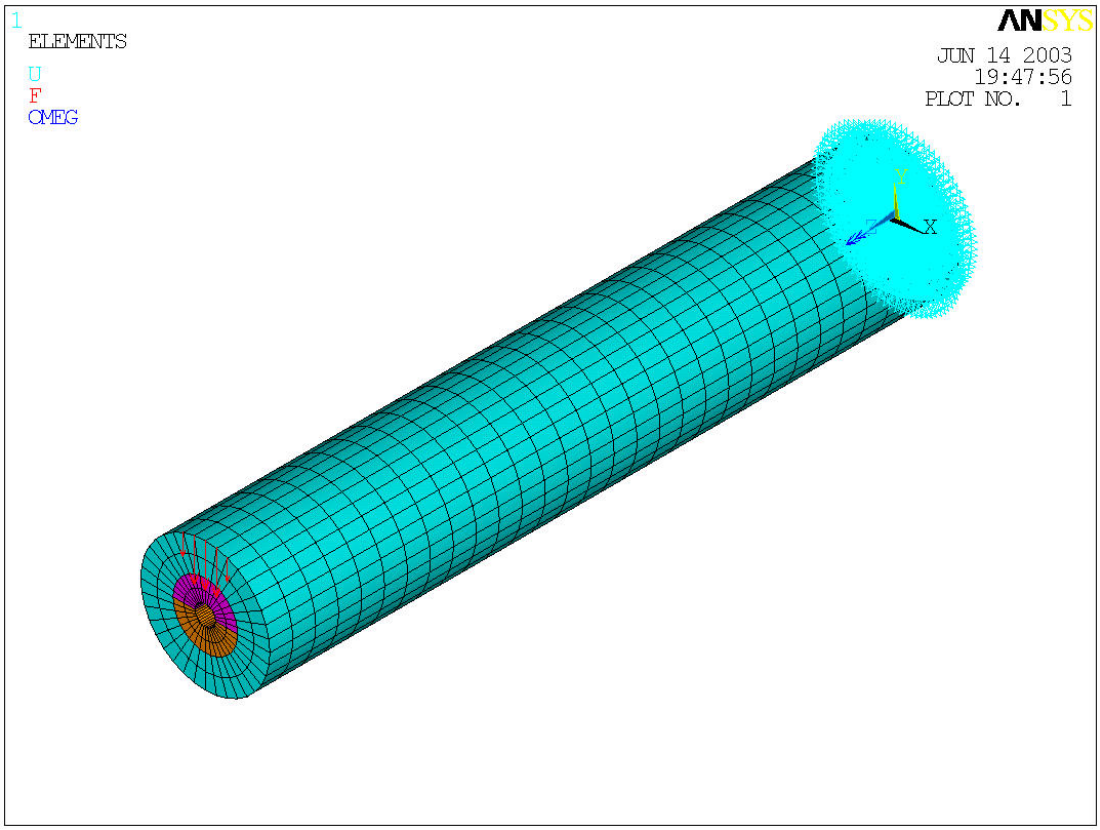


Figure 5-2. FEA model of the endmill using 20 node cubic elements and 8 node contact elements with boundary conditions.

Table 5-1. The number of nodes and elements.

| | |
|---|---|
| Node | 24826 |
| Element | 6480 |
| SOLID95 | 4320 |
| TARGE170 | 1080 |
| CONTA174 | 1080 |

Because the contact area is curved, higher order elements must be used to prevent inaccurate representation of the surface. Since the contact element is defined on the surface of solid elements, the consistent order of the element must be used for the structure and contact surface. The counter part of SOLID95 structural element is 8-node contact element, as illustrated in Fig.5-3. The contact elements are defined between the shank and finger.

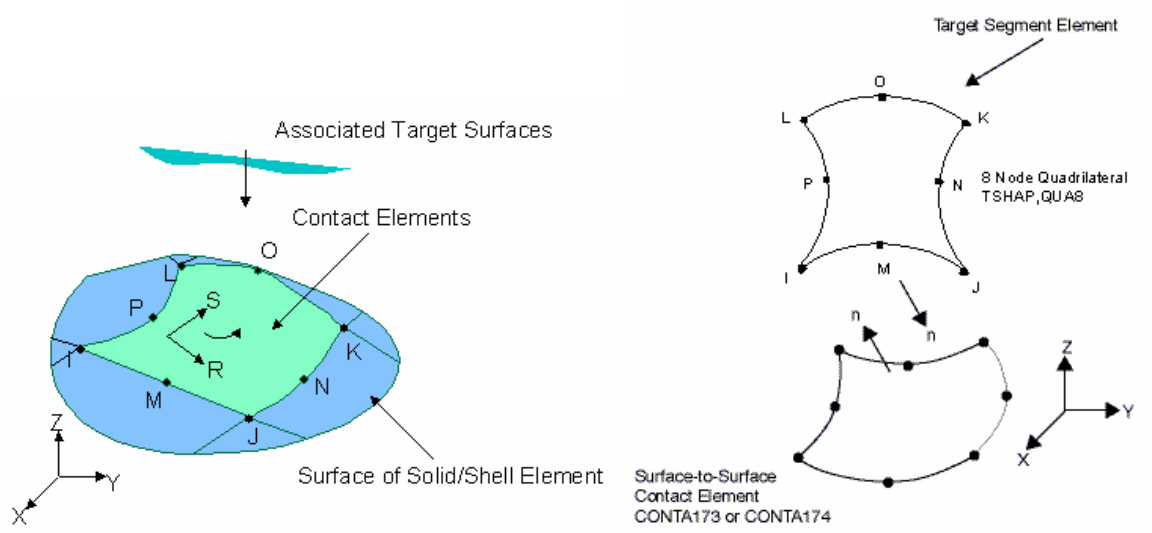


Figure 5-3. 8-node contact (CONTA174) and target (TARGE170) element description.

ANSYS offers CONTA174 and TARGE170 for contact and target elements, respectively. CONTA174 is used to represent the contact and sliding between 3-D "target" surfaces and a deformable surface, defined by this element. The element is applicable to 3-D structural and coupled thermal-structural contact analysis. This element is located on the surfaces of 3-D solid or shell elements with midside nodes. It has the same geometric characteristics as the solid or shell element face with which it is connected. Contact occurs when the element surface penetrates one of the target segment elements on a specified target surface. Coulomb and shear stress friction is allowed.

TARGE170 is used to represent various 3-D target surfaces for the associated contact elements. The contact elements themselves overlay the solid elements describing the boundary of a deformable body and are potentially in contact with the target surface, defined by TARGE170. This target surface is discretized by a set of target segment elements (TARGE170) and is paired with its associated contact surface via a shared real constant set. Any translational or rotational displacement, temperature, and voltage on the target segment element can be imposed. Forces and moments on target elements can also be imposed.

**Boundary Conditions**

According to the forces applied to the endmill, we can divide the analysis procedure into two steps. The first step is when the endmill starts rotating. In this step, only the angular velocity of 2,722.713 $[rad/\text{sec}]$ is applied without considering the cutting force.

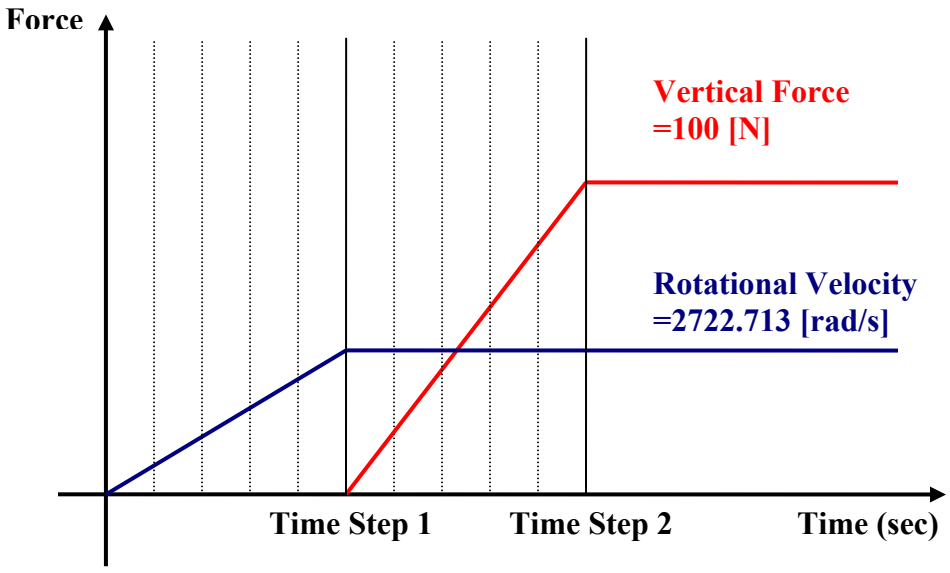


Figure 5-4. Force boundary conditions in each time step. Each time step is divided into 5 steps.

The second step is when the endmill starts the cutting process. At this time a vertical force of 100 N is applied at the tip of the endmill. Figure 5-4 illustrates the force boundary conditions in each step. Each time step is divided into 5 substeps in order to improve the convergence of nonlinear analysis.

**Calculation of Friction Work**

Even if the structure is linear elastic, the contact constraints make the problem nonlinear. In ANSYS, a Newton-Raphson iterative method is employed to solve the nonlinear system of equations. All default parameters in ANSYS are used in nonlinear analysis.

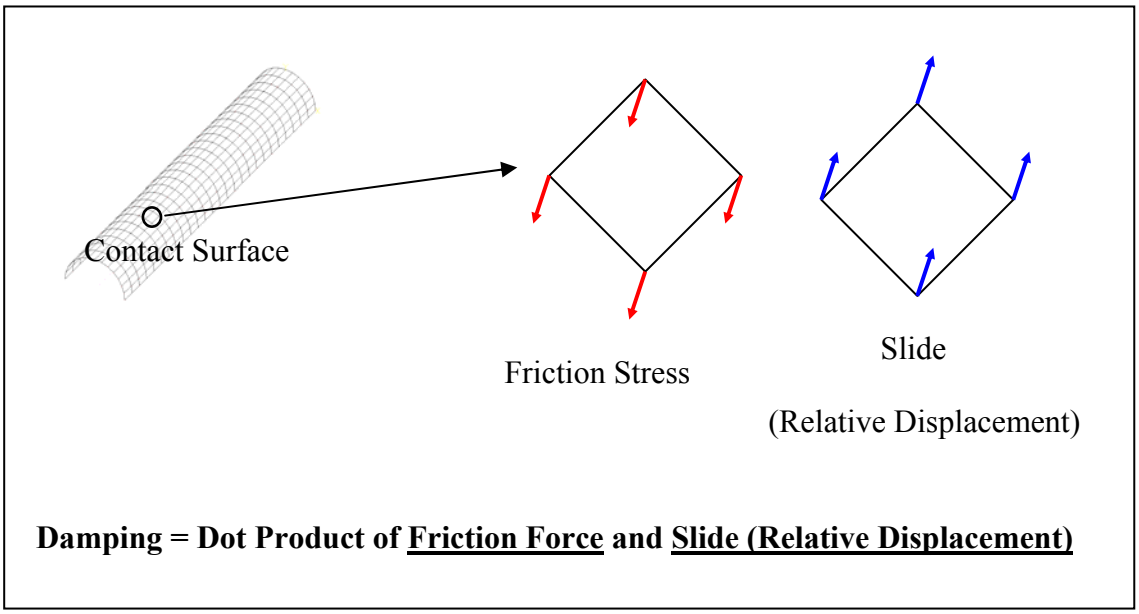


Figure 5-5. Diagram explaining how to calculate the damping work.

After finishing FEA, the damping work which is done by the friction force is calculated. The input commands to ANSYS for obtaining the frictional work are listed in Appendix D. Figure 5-5 shows a schematic procedure of the calculation. First, the friction stress and the relative slide in each contact element are obtained for each load step. By assuming a constant stress within an element, the friction force can be obtained by

multiplying the friction stress with the element area. The dot product of the friction force vector and the relative displacement vector in each substep and in each element yields the friction work.

## Finite Element Analysis Results

### Load Step 1

Figure 5-6 is the results at load step 1 when only the angular velocity is applied. In Chapter 3, the analytical method estimates the contact pressure to be 0.27[*MPa*].

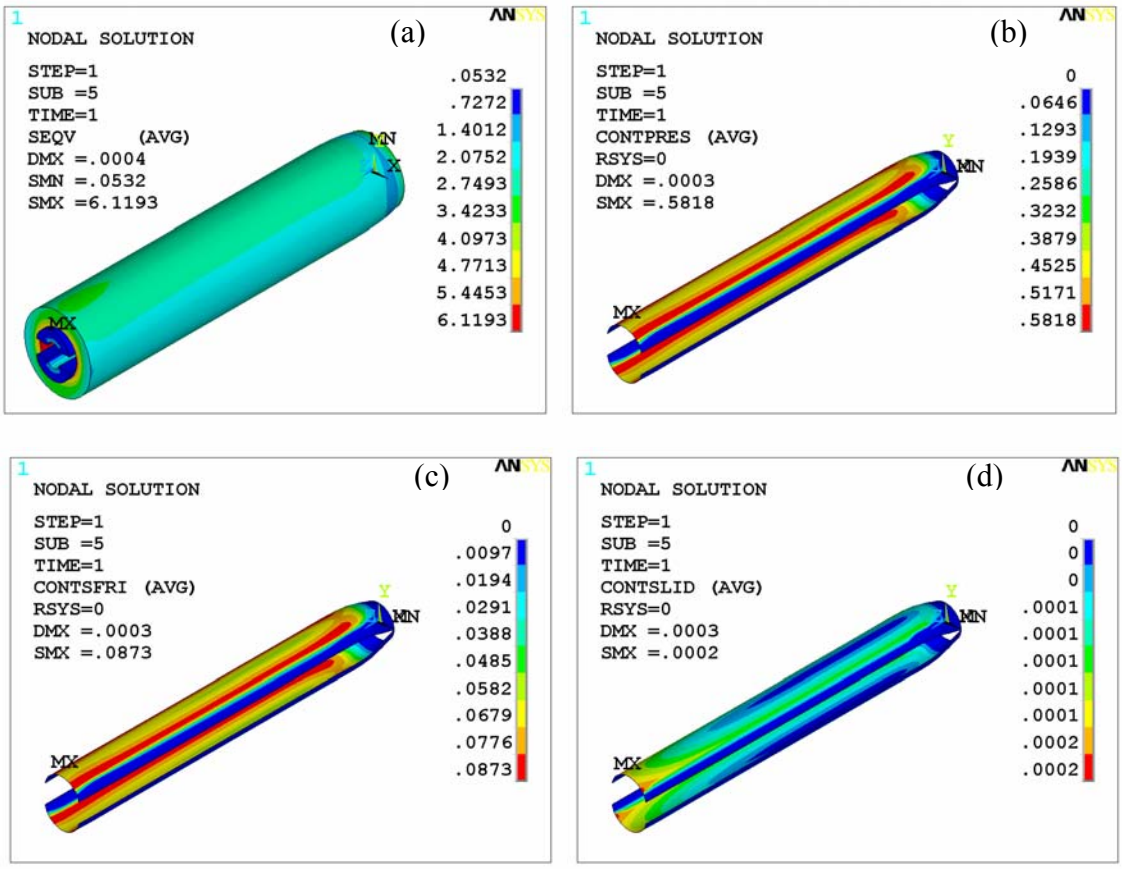


Figure 5-6. FEA result for load step 1 when only the angular velocity is applied. (a) is the von misses stress (MPa), (b) is the contact pressure (MPa), (c) is the frictional stress (MPa), and (d) is the slide (mm). MX indicates where the maximum value and MN means the minimum value.

Whereas, the maximum contact pressure from FEA is $0.58[MPa]$, as shown in Fig.5-6 (b). Since the actual contact occurs only half of the contact surface, the higher contact pressure from FEA is expected. In addition, the contact pressure is not constant: maximum at the top and the bottom surface and zero at both sides. Even though we assume that there is no relative motion between the contact surfaces during load step 1 in Chapter 3, there is a relative motion due to the diameter change. However, the relative motion in load step 1 should not be counted because it is not related to the chatter vibration.

**Load Step 2 (Centrifugal Force + Vertical Force)**

In the load step 2, a vertical force (cutting force) is applied on top of the centrifugal force. Figure 5-7 shows the results of load step 2. The frictional work is calculated by dot producing the friction force (Fig.5-7 (c)) and the relative slide (Fig.5-7 (d)). Since the load step is divided into five sub steps, the friction work at each sub step must be summed. The total friction work during load step 2 is $3.3426\times10^{-5}[J]$. By comparing with the analytical results $7.1182\times10^{-5}[J]$ in Chapter 3, the finite element analysis estimates about 50% of the analytical result. The friction work calculated from FEA is less than that from the analytical approach because the actual contact area is small in FEA. There is no contact on two sides: the neutral axis lies and the fixed end. In addition, the contact pressure is not constant. That is why the analytical result is about two times higher than the FEA result. Another interesting observation is that most of the relative displacement occurs on the bottom side of the finger (see Fig.5-7 (d)). That happens because the vertical force is applied to the top side of the endmill.

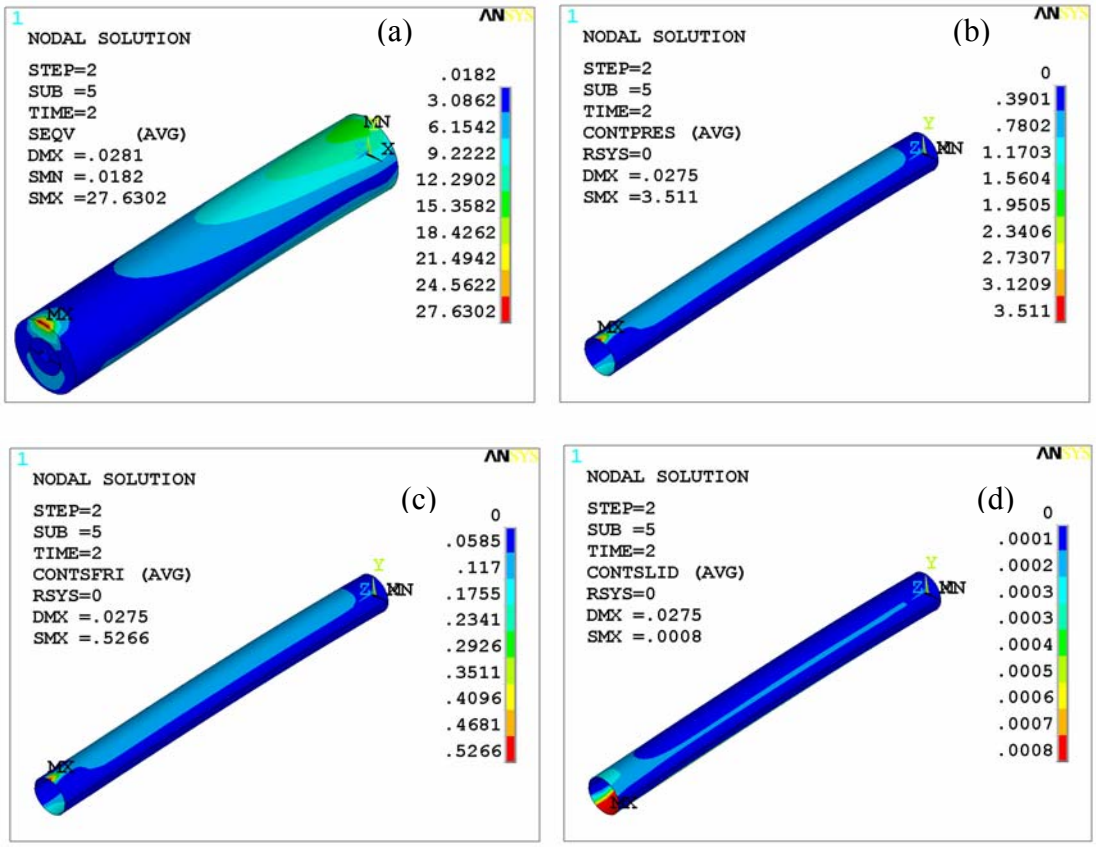


Figure 5-7. FEA result for load step 2 when both ngular velocity and vertical force are applied. (a) is the von misses stress (MPa), (b) is the contact pressure (MPa), (c) is the frictional stress (MPa), and (d) is the slide (mm). MX indicates where the maximum value and MN means the minimum value.

Figure 5-8, a schematic diagram of endmill bending according to the applied force, explains in more detail. This figure is exaggerated; the real deformation is very small. Fig.5-8 (a) shows the initial state. When the endmill starts rotating, the centrifugal force is applied and the deformed shape looks like Fig.5-8 (b). Due to the mass conservation, the length of the shank reduces as the diameter increases. Whereas, the length of the finger is not reduced because the cylindrical finger is cut along its neutral axis. When the vertical load is applied on top of the centrifugal force, the shank and the finger are deformed, as illustrated in Fig.5-8 (c). Due to the difference in geometric center, the deflected shape has the largest slide at the bottom surface.

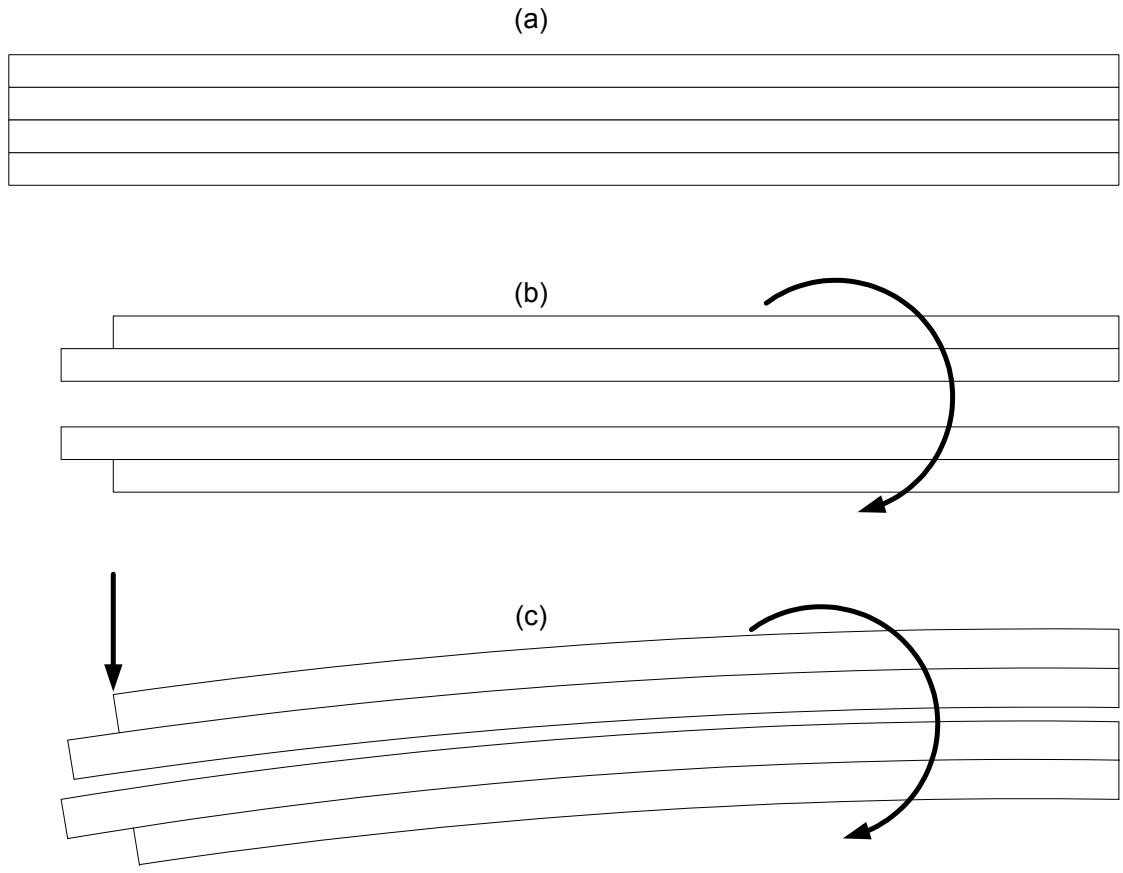


Figure 5-8.Schematic diagram of endmill behavior according to the applied forces. (a) shows the initial state, in (b) the angular velocity is applied and in (c) the vertical force is added.

# CHAPTER 6
# PARAMETER STUDY

In this chapter, a parameter study is performed to find the maximum value of the damping work. Two design variables, the inner radius of the finger and the number of the fingers, are changed. The results of the parameter study are discussed with respect to the results of the analytical approach.

## Determination of the Mesh Size

It is very important to determine the proper mesh size. A fine mesh will usually give an accurate result, but it requires a large amount of computational cost. Since the finite element analysis needs to be repeated 45 times during the parameter study, computational cost is an important issue.

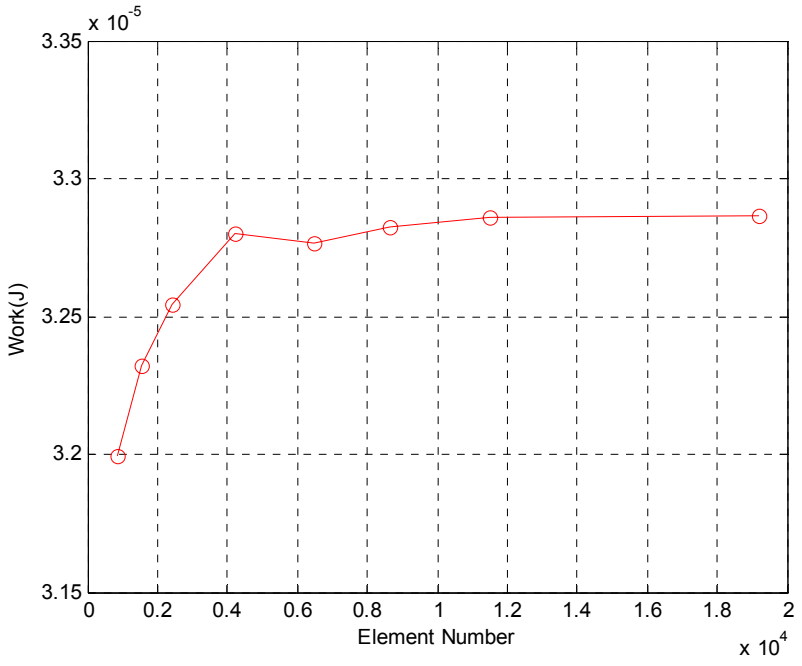


Figure 6-1. Damping according to the number of elements. Number of fingers = 2, inner radius R1=1mm, and start angle $\alpha = 0$.

Figure 6-1 shows the damping work according to the change of the number of elements. The work gradually increases until the element number reaches 4200, and then it converges on $3.28\times10^{-5}[J]$. Based on these results the number of elements is chosen to be 4200.

**Determination of the Start Angle.**

Before starting the parameter study, a start angle must be chosen for different configurations. This is because the damping value changes with starting angle even if the same number of fingers is used.

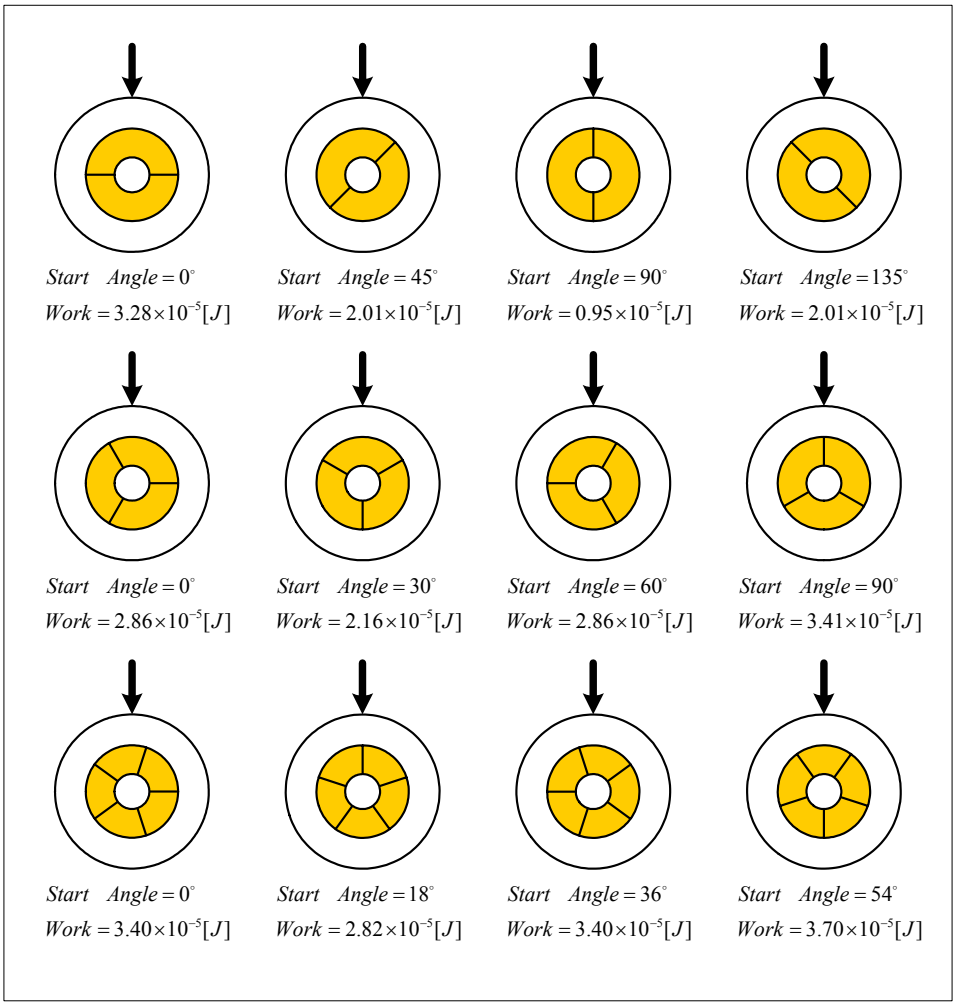


Figure 6-2. Damping according to the position of the finger

Figure 6-2 illustrates the difference of damping work according to the finger's position. The magnitude of damping work is different for different start angle. Thus, it is necessary to evaluate the maximum and minimum values together. Figure 6-3 is the plot of the minimum and maximum values for the same number of fingers when the inner radius is 1.0 mm. The results show a large difference between the minimum and maximum values when the number of fingers is small. However the difference is reduced as the number of fingers is increased. If we compare this result with the analytical result, shown in Fig.3-6, the FEA estimated damping work converges to a third of analytical damping work. Possible explanations are from the fact that not all portion of the fingers are in contact and the relative slide is large at the bottom surface.

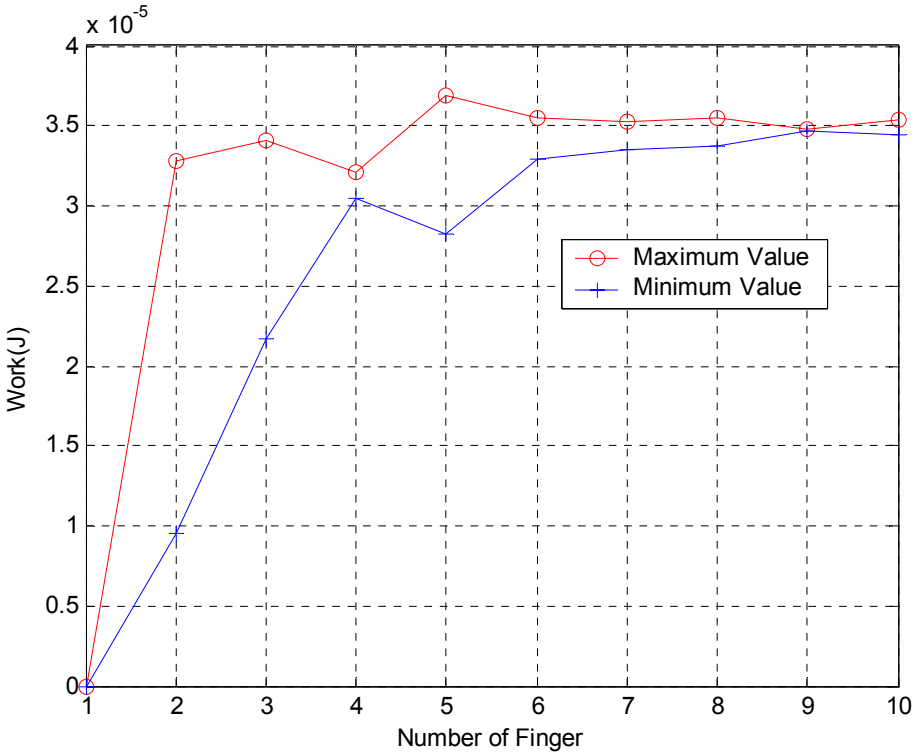


Figure 6-3. The maximum and the minimum values of the damping work for the given number of fingers.

Let us consider the cases where the number of fingers is 2 and 5 more in detail. Figure 6-4 shows the relative displacement for the two-finger case. Figure 6-4 (a) and (b) show the case where the start angle of the finger is $90^\circ$. Fig.6-4 (c) and (d) show the result when the start angle is $0^\circ$. In both cases the pressure between the contact surfaces is almost the same for each position of the finger. But the relative displacement is different.

(a) Top

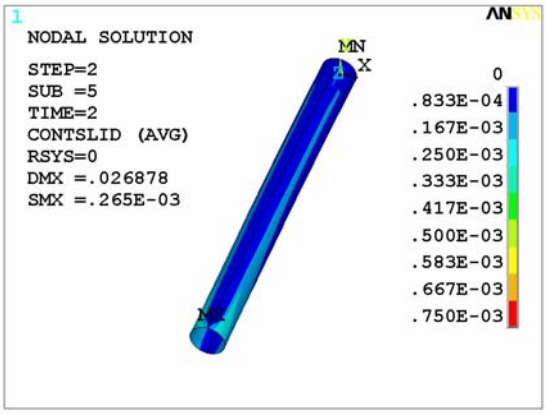


(b) Bottom

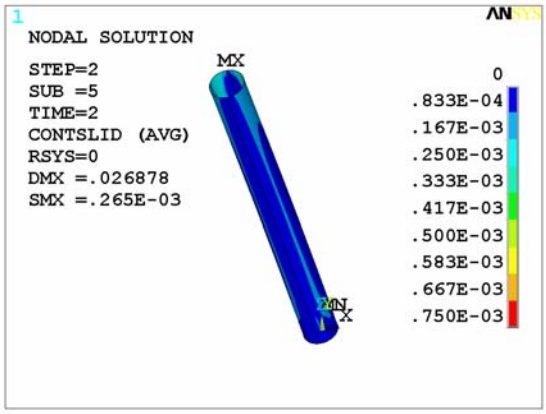


(c) Top

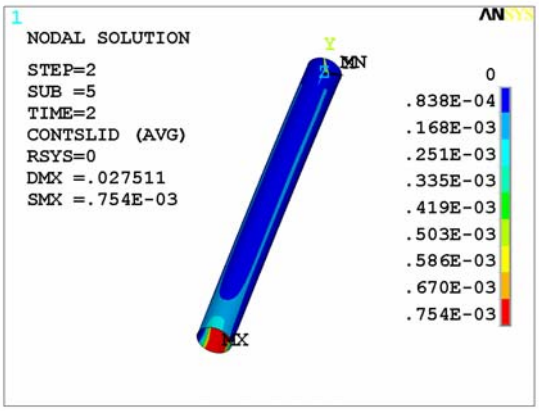


(d) Bottom

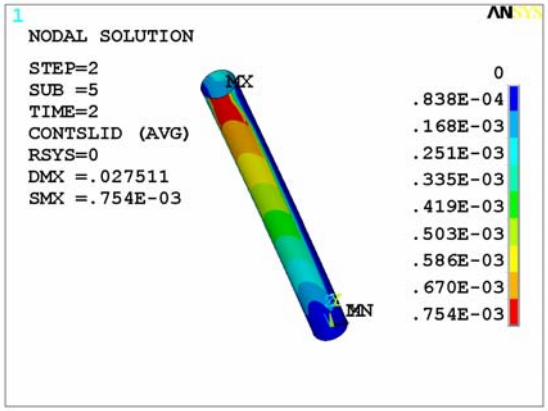


Figure 6-4. Relative displacement of the two-finger case. (a), (b) is when the start angle of the finger is $90^\circ$, and (c), (d) is $0^\circ$. MX indicates where the maximum value occurs and MN means the minimum value.

The figure shows that most sliding occurs in the bottom part of the contact surface. That is because the force is applied at the top surface. If we use this relative displacement

for calculating the frictional work, the work calculated when the start angle is $0^{\circ}$ is bigger than $90^{\circ}$.

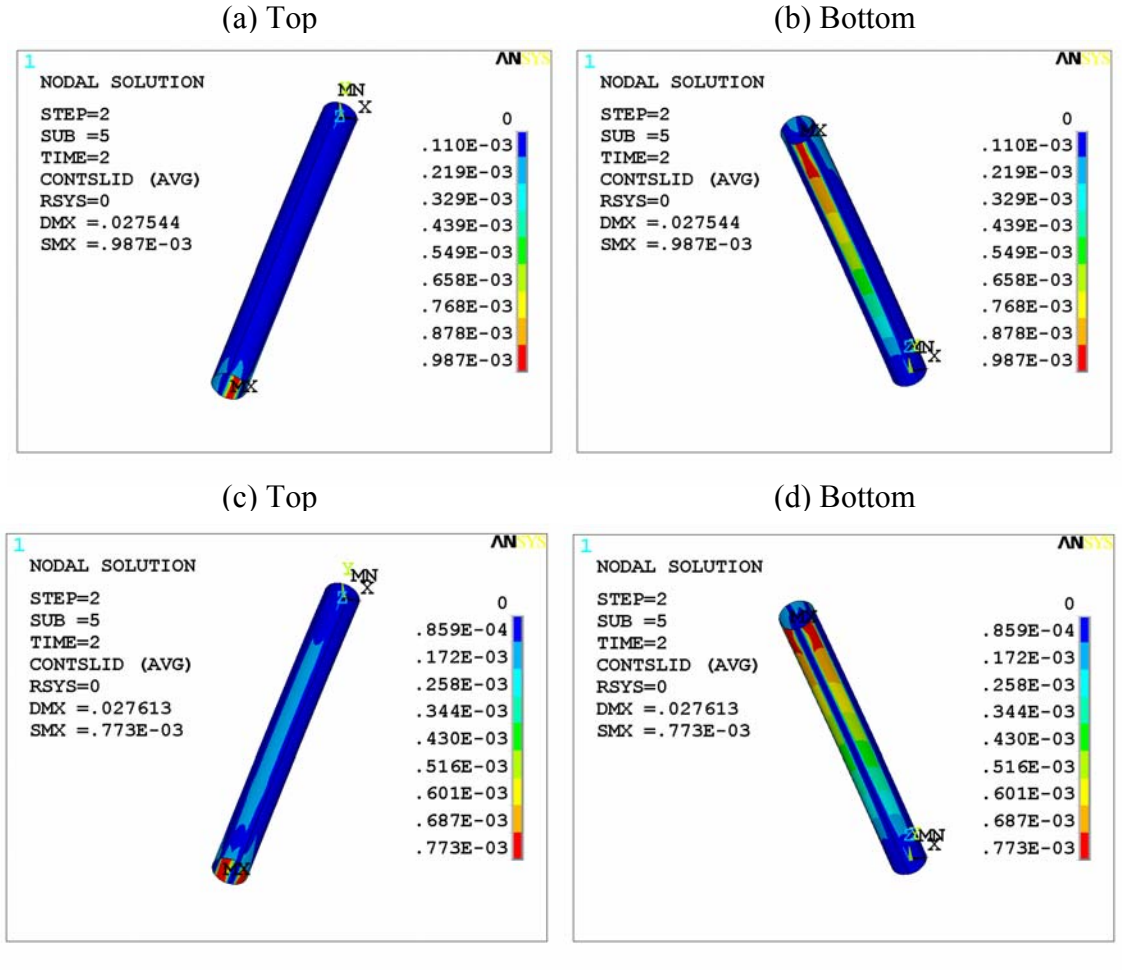


Figure 6-5. Relative displacement of five-finger case. (a), (b) is when the start angle of the finger is $18^{\circ}$, and (c), (d) is $54^{\circ}$. MX indicates where the maximum value occurs and MN means the minimum value.

The five-finger case is very similar to the two-fingered case. Figure 6-5 shows the five-finger case. Parts (a) and (b) are for a start angle of $18^{\circ}$ and parts (c) and (d) are for a start angle of $54^{\circ}$. If we compare Fig.6-5 (b) with Fig.6-5 (d), the latter has almost twice greater sliding region than the former. This is because the location of the finger differently affects the damping work. However, Fig.6-3 shows that these effects

disappear as the number of fingers increases. This means that when the number of fingers is small the work done by the friction force depends on the start angle.

**Parameter Study**

To find the maximum value of damping, a parameter study was done for two design variables. Figure 6-6 shows the first design variable, which is the inner radius of the finger, and Fig.6-7, the second design variable, the number of fingers.

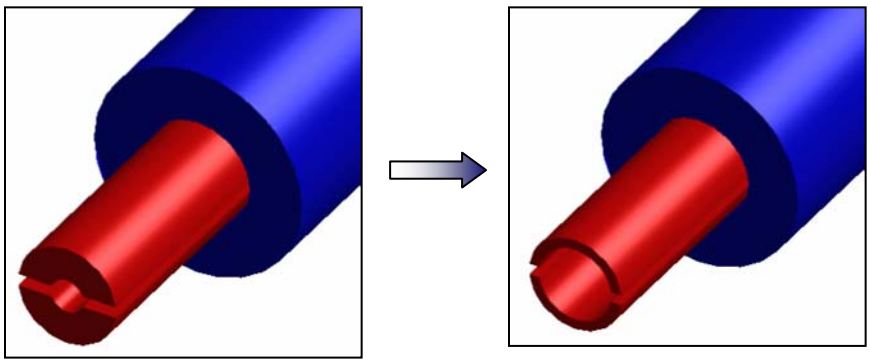

Figure 6-6. The first design variable: the inner radius (R1) of the finger (varied from 1.5 mm to 3.5 mm).

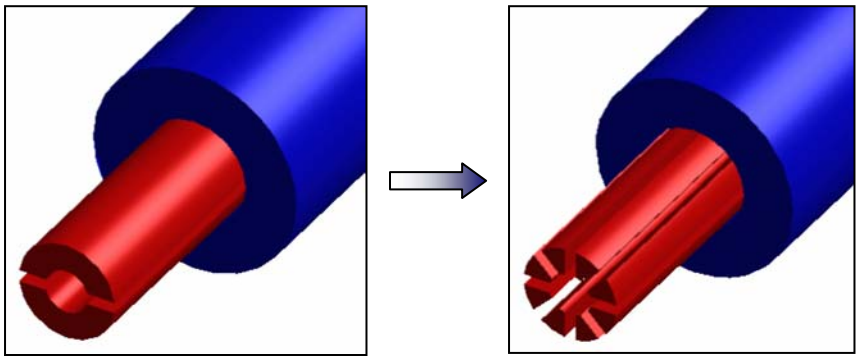

Figure 6-7. The second design variable: the number of fingers (from 2 to 10).

**Change the Inner Radius of the Finger.**

First the radius is changed from 1.0mm to 3.5mm for the two-finger case. Figure 6-8 shows the result.

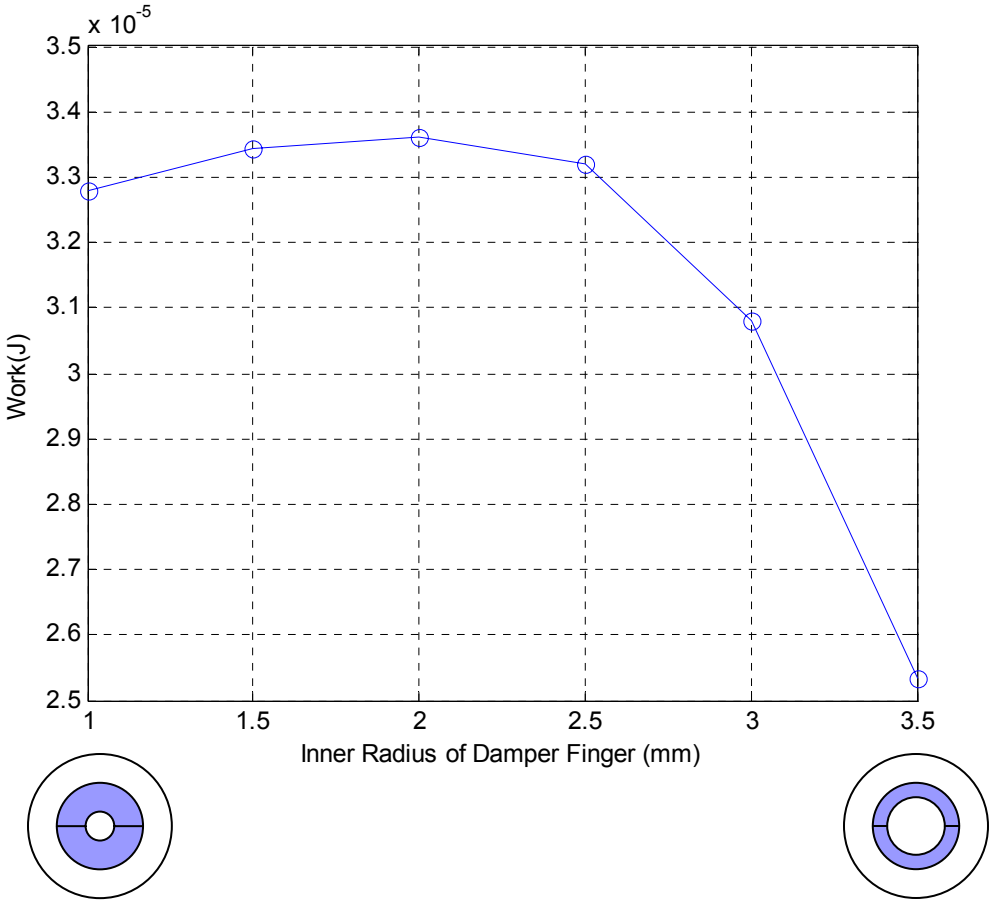


Figure 6-8. The result of the parameter study in which the inner radius of finger was changed.

It's obvious that the work done by the friction force is gradually reduced, since the mass of the finger is reduced when the radius is reduced. When the radius is 1.0mm the damping is $3.28\times10^{-5}[J]$, and when the radius is 3.5mm it is $2.53\times10^{-5}[J]$.

**Change the Number of the Finger**

Next the number of fingers is changed from 2 to 10 for the case where the inner radius is 1.5 mm. The damping work shows a minimum value for the four-finger case, and a maximum value for the five-fingered case. The start angle of the finger (position of the finger) is chosen to have the maximum damping.

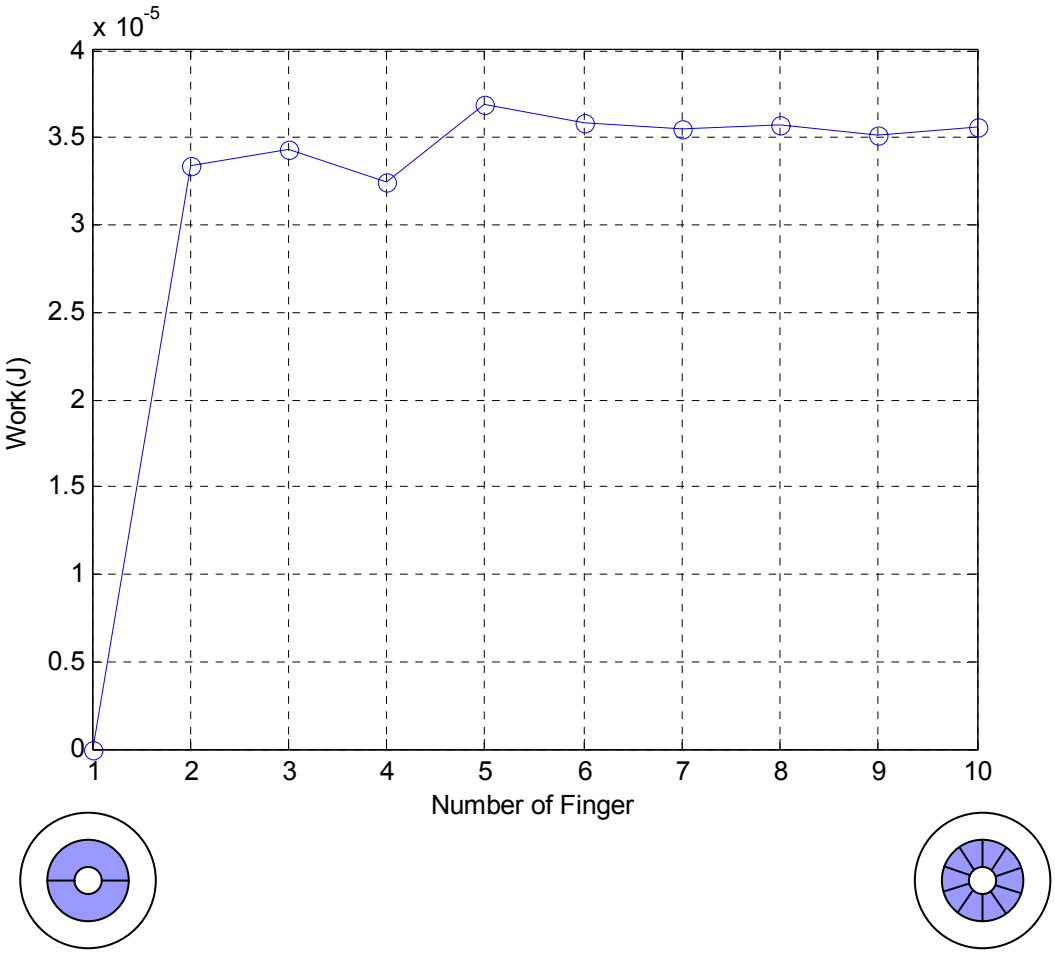


Figure 6-9. The result of the parameter study in which the number of fingers was changed.

**Final Results**

The parameter study is repeated for all cases, and the results are as follows.

Table 6-1. The results of parameter study $\times 10^{-5}$ [J]

| | 2 | 3 | 4 | 5 | 6 | 7 | 8 | 9 | 10 |
|---|---|---|---|---|---|---|---|---|---|
| 1.0 mm | 3.28 | 3.41 | 3.21 | 3.69 | 3.55 | 3.54 | 3.54 | 3.48 | 3.51 |
| 1.5 mm | 3.34 | 3.43 | 3.24 | 3.72 | 3.58 | 3.55 | 3.57 | 3.52 | 3.56 |
| 2.0 mm | 3.36 | 3.41 | 3.24 | 3.69 | 3.54 | 3.47 | 3.52 | 3.45 | 3.50 |
| 2.5 mm | 3.31 | 3.31 | 3.18 | 3.57 | 3.36 | 3.33 | 3.39 | 3.35 | 3.42 |
| 3.0 mm | 3.08 | 3.10 | 3.02 | 3.32 | 3.10 | 3.08 | 3.12 | 3.04 | 3.16 |
| 3.5 mm | 2.53 | 2.62 | 2.65 | 2.83 | 2.61 | 2.63 | 2.65 | 2.60 | 2.68 |

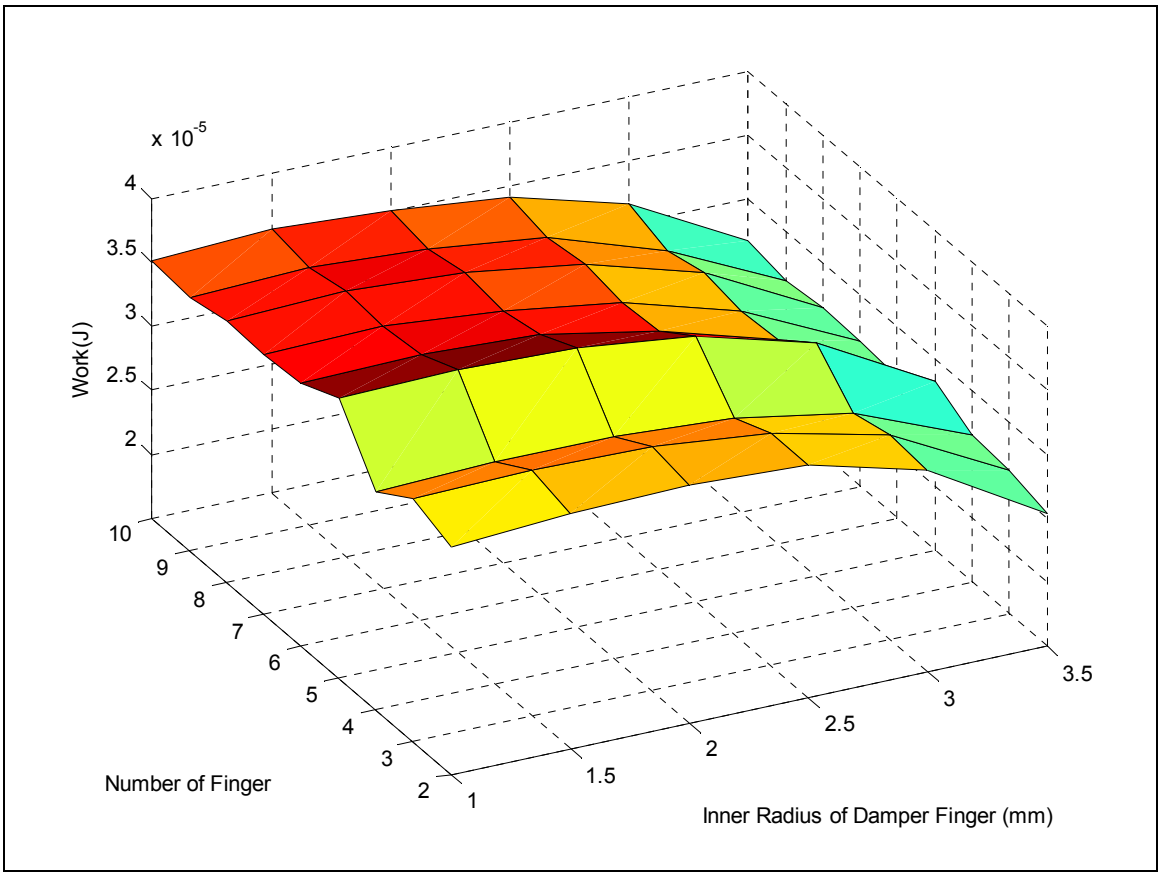


Figure 6-10. The plot of the Table 6-1.

In order to find the configuration that yields the maximum damping work, the first design variable (R1) is changed by six different values and the second design variable (number of finger) is changed by nine different values. Table 6-1 shows the results in 6×9 matrix. In each configuration, the start angle is chosen such that the maximum damping work can be occurred. Figure 6-10 plots the response surface of the damping work. Even if the second design variable is discrete, a continuous surface is plotted for illustration purpose. It is noted that the local peak when the number of fingers is five is maintained throughout all different radii. The general trend of the response surface is consistent. Based on the response surface, we can conclude that the damping work has its maximum value when the inner radius is 1.5 mm and the number of fingers is 5. However, the large

difference in maximum and minimum damping values in this configuration, as shown in Fig.6-3, may reduce the significance of this choice of design.

As a conclusion, the effect of damping work increases as the number of fingers is increased and the inner radius is decreased.

**Comparison between the Analytical and Numerical Results**

Figure 6-9 shows the analytical and numerical results of friction work as a function of the number of fingers. The friction work estimated from finite element analysis is less than half of the friction work obtained from the analytical method. The possible explanations of such discrepancy are the assumption of constant contact pressure.

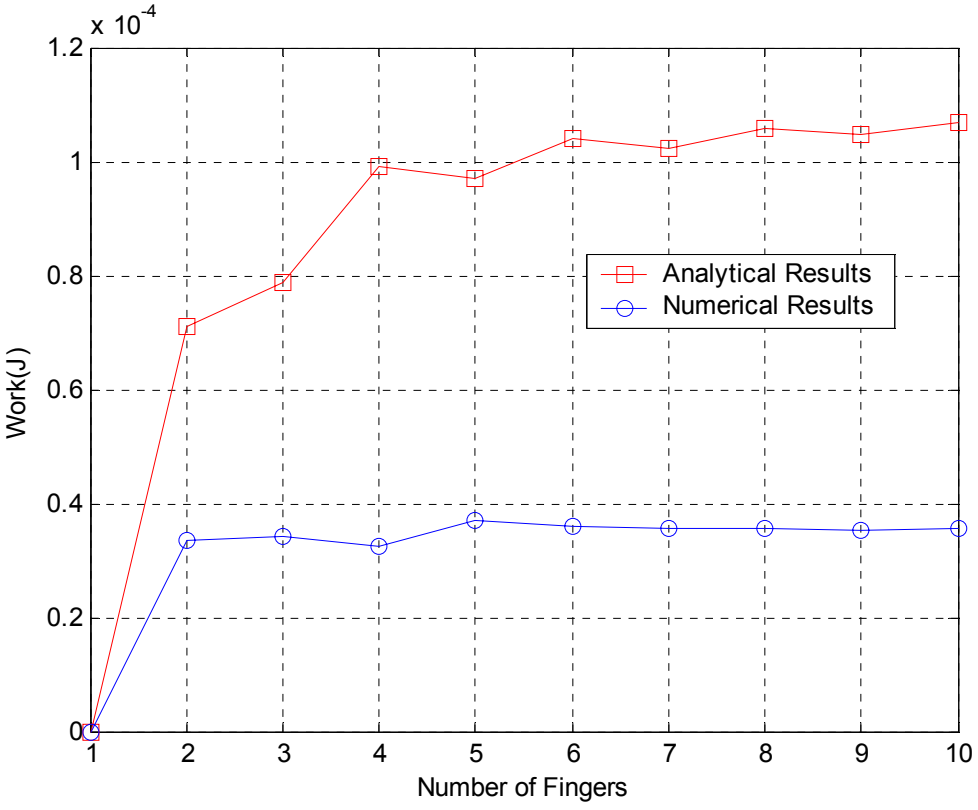


Figure 6-9. Plot of the analytical and numerical resutls.

In reality, the contact pressure is not constant and same portion of the finger does not contact with the shank. And most relative motion occurs at the bottom part of the

endmill. That is because the vertical force is applied at the top and the nonlinearity associated with the centrifugal force contributes the asymmetry between the top and bottom fingers. During the nonlinear analysis ANSYS automatically update the geometry and refer to the deformed configuration, which means the body force is calculated at the deformed geometry. Even though the analytical and numerical results show the difference, the general trends of both results are very similar each other.

In order to explain the general trends of friction work, consider the analytical explanation of the contact pressure:

$$P_c = \frac{MR\omega^2}{A_c},$$

where $\frac{M}{A_c}$ and $\omega$ is constant. Value $R$, which is the distance between the rotational center and the mass center of the finger, can be calculated by

$$R = \frac{2\left(R_2^{\,3} - R_1^{\,3}\right)}{3\left(R_2^{\,2} - R_1^{\,2}\right)} \frac{\sin(\alpha)}{\alpha}$$

If we assume that the friction work is proportional to the contact pressure, then the friction work is proportional to $R$, which increases as the number of fingers increases. If the number of the finger increases, which means the angle $\alpha$ goes to zero, $R$ is converges to

$$R = \frac{2\left(R_2^{\,3} - R_1^{\,3}\right)}{3\left(R_2^{\,2} - R_1^{\,2}\right)}$$

Therefore, the maximum value of the contact pressure can be calculated by

$$P_c = \frac{MR\omega^2}{A_c} = \frac{2\left(R_2^{\,3} - R_1^{\,3}\right)}{3\left(R_2^{\,2} - R_1^{\,2}\right)} \frac{M\omega^2}{A_c}$$

As a conclusion, the friction work increases along with the number of fingers, but its effect is reduced as the number of fingers increases.

# CHAPTER 7
# CONCLUSION AND FUTURE WORK

The goal of this research was to design the mechanical damper which is inserted into the endmill. Through the nonlinear finite element analysis and parameter study, the trend of the damping effect is identified.

The results from the analytical method were used to verify the FEA result. Although the number and the inner radius of finger were varied in finite element analysis, only the two-finger case was considered in the comparison. The FEA results were smaller than those of the analytical approach because some regions did not contact and the contact pressure was not constant.

A parameter study was carried out by changing the inner radius and the number of fingers. The inner radius was varied from 1.0 mm to 3.5 mm, and the number of fingers was varied from 2 to 10. The results show general trends of the damping work according to the change of the two design variables. As the inner radius decreased and the number of finger increased, the damping work increased. The Maximum value was $3.72\times10^{-5}[J]$ when the inner radius was 1.5 mm and the number of fingers was 5. The parameter study also showed that when the number of the fingers is small the damping work is affected by the position of the finger, but that this dependence disappears as the number of finger increases.

## Recommendations for Future Research

As discussed in Chapter 6, the damping work depends on the start angle. However, in practice the endmill is continuously rotating. Thus, it is recommended to perform a

series of static FEA by rotating the endmill by on cycle and to calculate the integrated damping work. This procedure will provide more accurate estimation of the real damping work.

APPENDIX A
MATLAB CODE FOR THEORITICAL ANALYSIS

```
%-------------------------------------------------------------------------------
% Matlab function to calculate the work done by the friction force
%
%                                                    By Dongki Won
%-------------------------------------------------------------------------------
function cal_work
%-------------------------------------------------------------------------------
% Material Properties, radius and applied forces.
%-------------------------------------------------------------------------------
E=2.0678e11;        %- Modulus of Elasticity : 2.0*10^11[MPa]
rho=7820;           %- Mass Density : 7820[kg/m^3]
mu=0.15;            %- Friction Coefficient : 0.15
r1=1.5e-3;
r2=4.7625e-3;
r3=r2;
r4=9.525e-3;
L=101.6e-3;
omega=2722;
F=100;
%-------------------------------------------------------------------------------
% Calculate the work according to the chage of the inner raius of finger.
%-------------------------------------------------------------------------------
n=2;m=1;
for r1=1.0e-3:0.5e-3:3.5e-3
   ang(1)=0;
   for i=1:n
      ang(i+1)=ang(1)+(360/n)*i;
   end
   ang=ang*(pi/180);
   II=(1/4)*((r4)^4-(r3)^4)*pi;
   for i=1:(n-1)
      tmp1=sin(ang(i+1))*cos(ang(i+1))-sin(ang(i))*cos(ang(i))-(ang(i+1)-ang(i));
      tmp1=tmp1*((r1)^4-(r2)^4);
      tmp1=tmp1*(1/8);
      II=II+tmp1;
   end
   work=0;
   for i=1:n
      alpha=(ang(i+1)-ang(i))/2;
```

```
      d1=(2*sin(alpha).*(r2^3-r1^3))/(3*alpha*(r2^2-r1^2));
      d2=d1*sin((ang(i)+ang(i+1))*0.5);
      V=(ang(i+1)-ang(i))*(r2^2-r1^2)*L*0.5;
      P=abs(V*rho*(omega^2)*d1/L);
      work=work+abs((1/3)*(L^3)*mu*P*F*d2/(E*II));
   end
   y1(m)=work;
   m=m+1;
end
x1=[1.0e-3:0.5e-3:3.5e-3];
plot(x1,y1,'b-o');
grid;
xlabel('Inner Radius of Damper Finger (m)');
ylabel('Work(J)');
[tmp,n]=size(x1);
clc
fprintf('\nCalculate the work according to the chage of the inner raius of finger.\n');
fprintf('The Number of Finger=%3.0f\nStart Angle=%3.0f [Degree]\n',n,0);
for i=1:n
   fprintf('Inner Raius of Finger =%16.9e [m]\t\tWork=%16.9e [J]\n',x1(i),y1(i));
end
%-------------------------------------------------------------------------------
% Calculate the work according to the chage of the start angle of finger.
%-------------------------------------------------------------------------------
n=2;m=1;r1=1.5e-3;
atmp=(360/n)/4;
for a=0:atmp:atmp*3
   ang(1)=a;
   for i=1:n
      ang(i+1)=ang(1)+(360/n)*i;
   end
   ang=ang*(pi/180);
   II=(1/4)*((r4)^4-(r3)^4)*pi;
   for i=1:(n-1)
      tmp1=sin(ang(i+1))*cos(ang(i+1))-sin(ang(i))*cos(ang(i))-(ang(i+1)-ang(i));
      tmp1=tmp1*((r1)^4-(r2)^4);
      tmp1=tmp1*(1/8);
      II=II+tmp1;
   end
   work=0;
   for i=1:n
      alpha=(ang(i+1)-ang(i))/2;
      d1=(2*sin(alpha).*(r2^3-r1^3))/(3*alpha*(r2^2-r1^2));
      d2=d1*sin((ang(i)+ang(i+1))*0.5);
      V=(ang(i+1)-ang(i))*(r2^2-r1^2)*L*0.5;
      P=abs(V*rho*(omega^2)*d1/L);
```

```
      work=work+abs((1/3)*(L^3)*mu*P*F*d2/(E*II));
   end
   y2(m)=work;
   m=m+1;
end
x2=[0:atmp:atmp*3];
figure;
plot(x2,y2,'b-o');
grid;
xlabel('Start Angle of Damper Finger (degree)');
ylabel('Work(J)');
[tmp,n]=size(x2);
fprintf('\nCalculate the work according to the chage of the start angle of finger.\n');
fprintf('Number of Finger=%5.0f\nInner Radius of the Finger=%16.9e [m]\n',2,r1);
for i=1:n
   fprintf('Start Angle =%16.9e [Degree]\t\tWork=%16.9e [J]\n',x2(i),y2(i));
end
%--------------------------------------------------------------------------------
% Calculate the work according to the change of the number of finger.
%--------------------------------------------------------------------------------
m=1;clear ang
for n=2:10
   clear ang
   atmp=(1+(-1)^(n-1))/2;
   ang(1)=((360/n)/4)*atmp;
   for i=1:n
      ang(i+1)=ang(1)+(360/n)*i;
   end
   ang=ang*(pi/180);
   II=(1/4)*((r4)^4-(r3)^4)*pi;
   for i=1:(n-1)
      tmp1=sin(ang(i+1))*cos(ang(i+1))-sin(ang(i))*cos(ang(i))-(ang(i+1)-ang(i));
      tmp1=tmp1*((r1)^4-(r2)^4);
      tmp1=tmp1*(1/8);
      II=II+tmp1;
   end
   work=0;
   for i=1:n
      alpha=(ang(i+1)-ang(i))/2;
      d1=(2*sin(alpha).*(r2^3-r1^3))/(3*alpha*(r2^2-r1^2));
      d2=d1*sin((ang(i)+ang(i+1))*0.5);
      V=(ang(i+1)-ang(i))*(r2^2-r1^2)*L*0.5;
      P=abs(V*rho*(omega^2)*d1/L);
      work=work+abs((1/3)*(L^3)*mu*P*F*d2/(E*II));
   end
   y3(m+1)=work;
```

```
   m=m+1;
end
x3=[1:10];
figure;
plot(x3,y3,'b-o');
axis([0,10,0,11e-5]);
grid;
xlabel('Number of Damper Finger');
ylabel('Work(J)');
[tmp,n]=size(x3);
fprintf('\nCalculate the work according to the chage of the number of finger.\n');
fprintf('Inner Radius of the Finger=%16.9e [m]\n',r1);
for i=1:n
   fprintf('Number of Finger =%3.0f\t\tWork=%16.9e [J]\n',x3(i),y3(i));
end
```

APPENDIX B
ANSYS INPUT FILE 01

```
!-------------------------------------------------------------------------------
!   ANSYS input file to determine the mesh size according to the change of
! elemnt number. The results are stored in mesh_size,txt.
!
!                    Dongki Won
!-------------------------------------------------------------------------------
/SHOW,JPEG

*SET,rad_in,1.5              ! Inner radius of the finger
*SET,rad_out1,4.7625         ! Outer radius of the finger
*SET,rad_out2,9.525          ! Outer radius of the shank
*SET,f_num,2                 ! The number of fingers
*SET,f_ang,360/f_num         ! The angle of one finger
*SET,st_ang,(f_ang/4)*0      ! Start angle of the finger

*DO,ii,1,8
  *IF,ii,EQ,1,THEN      ! Element Number is 864
    *SET,s_mesh,6
    *SET,f_mesh,6
    *SET,l_mesh,12
    *SET,st_mesh,2
    *SET,ft_mesh,2
  *ELSEIF,ii,EQ,2       ! Element Number is 1536
    *SET,s_mesh,8
    *SET,f_mesh,8
    *SET,l_mesh,16
    *SET,st_mesh,2
    *SET,ft_mesh,2
  *ELSEIF,ii,EQ,3       ! Element Number is 2400
    *SET,s_mesh,10
    *SET,f_mesh,10
    *SET,l_mesh,20
    *SET,st_mesh,2
    *SET,ft_mesh,2
  *ELSEIF,ii,EQ,4       ! Element Number is 4200
    *SET,s_mesh,14
    *SET,f_mesh,14
    *SET,l_mesh,25
    *SET,st_mesh,2
```

```
    *SET,ft_mesh,2
  *ELSEIF,ii,EQ,5      ! Element Number is 6480
    *SET,s_mesh,18
    *SET,f_mesh,18
    *SET,l_mesh,30
    *SET,st_mesh,2
    *SET,ft_mesh,2
  *ELSEIF,ii,EQ,6      ! Element Number is 8640
    *SET,s_mesh,18
    *SET,f_mesh,18
    *SET,l_mesh,30
    *SET,st_mesh,3
    *SET,ft_mesh,3
  *ELSEIF,ii,EQ,7      ! Element Number is 11500
    *SET,s_mesh,18
    *SET,f_mesh,18
    *SET,l_mesh,40
    *SET,st_mesh,3
    *SET,ft_mesh,3
  *ELSEIF,ii,EQ,8      ! Element Number is 19200
    *SET,s_mesh,20
    *SET,f_mesh,20
    *SET,l_mesh,60
    *SET,st_mesh,3
    *SET,ft_mesh,3
  *ENDIF
  tmp1=s_mesh*l_mesh*2*(1+st_mesh)
  tmp2=f_mesh*l_mesh*2*(1+ft_mesh)
  num_elem=tmp1+tmp2
  /INPUT,endmill_model,inp
  /INPUT,endmill_work,inp
  /OUTPUT,mesh_size,txt,,APPEND
  *VWRITE,num_elem,work
  (F7.0,3X,F16.9,3X)
  /OUTPUT
*ENDDO
```

APPENDIX C
ANSYS INPUT FILE 02

```
!-------------------------------------------------------------------------------------
!   ANSYS input file to determine the start angle of the finger.
! The results are stored in start_angle,txt.
!
!                    Dongki Won
!-------------------------------------------------------------------------------------
/SHOW,JPEG

*SET,rad_in,1                ! Inner radius of the finger
*SET,rad_out1,4.7625         ! Outer radius of the finger
*SET,rad_out2,9.525          ! Outer radius of the shank
*SET,s_mesh,14
*SET,l_mesh,30
*SET,st_mesh,2
*SET,ft_mesh,2

*DO,ii,8,10
  *SET,f_num,ii
  *SET,f_ang,360/f_num
  *IF,ii,EQ,2,THEN
    *SET,f_mesh,14
  *ELSEIF,ii,EQ,3
    *SET,f_mesh,9
  *ELSEIF,ii,EQ,4
    *SET,f_mesh,7
  *ELSEIF,ii,EQ,5
    *SET,f_mesh,6
  *ELSEIF,ii,EQ,6
    *SET,f_mesh,5
  *ELSEIF,ii,EQ,7
    *SET,f_mesh,4
  *ELSEIF,ii,EQ,8
    *SET,f_mesh,4
    *SET,s_mesh,16
    *SET,ft_mesh,2
  *ELSEIF,ii,EQ,9
    *SET,f_mesh,4
    *SET,s_mesh,18
    !*SET,ft_mesh,2
```

```
  *ELSEIF,ii,EQ,10
    *SET,f_mesh,3
    *SET,s_mesh,15
    !*SET,ft_mesh,3
  *ENDIF
  *DO,jj,0,3
    *SET,st_ang,(f_ang/4)*jj
    /INPUT,endmill_model,inp
    /INPUT,endmill_work,inp
    /OUTPUT,start_angle,txt,,APPEND
    *VWRITE,f_num,jj,st_ang,work
    (F7.0,3X,F7.0,3X,F16.9,3X,F16.9,3X)
    /OUTPUT
  *ENDDO
*ENDDO
```

APPENDIX D
ANSYS INPUT FILE 03

```
!-----------------------------------------------------------------------------------------
!   ANSYS input file to do the parameter study as the change of two design
! variables, the number of the finger(f_num) and the inner radius of the finger
! (rad_in). The results are stored in parameter_study,txt.
!
!                    Dongki Won
!-----------------------------------------------------------------------------------------
/SHOW,JPEG

*SET,rad_out1,4.7625        ! Outer radius of the finger
*SET,rad_out2,9.525         ! Outer radius of the shank
*SET,s_mesh,14
*SET,l_mesh,25
*SET,st_mesh,2
*SET,ft_mesh,2

*DO,ii,2,10
  *SET,f_num,ii
  *SET,f_ang,360/f_num
  *IF,ii,EQ,2,THEN
    *SET,f_mesh,14
    *SET,st_ang,(f_ang/4)*0
  *ELSEIF,ii,EQ,3
    *SET,f_mesh,9
    *SET,st_ang,(f_ang/4)*3
  *ELSEIF,ii,EQ,4
    *SET,f_mesh,7
    *SET,st_ang,(f_ang/4)*2
  *ELSEIF,ii,EQ,5
    *SET,f_mesh,6
    *SET,st_ang,(f_ang/4)*3
  *ELSEIF,ii,EQ,6
    *SET,f_mesh,5
    *SET,st_ang,(f_ang/4)*2
  *ELSEIF,ii,EQ,7
    *SET,f_mesh,4
    *SET,st_ang,(f_ang/4)*3
  *ELSEIF,ii,EQ,8
    *SET,f_mesh,4
```

```
    *SET,s_mesh,16
    *SET,st_ang,(f_ang/4)*2
  *ELSEIF,ii,EQ,9
    *SET,f_mesh,4
    *SET,s_mesh,18
    *SET,st_ang,(f_ang/4)*3
    *SET,ft_mesh,2
    *SET,l_mesh,30
  *ELSEIF,ii,EQ,10
    *SET,f_mesh,3
    *SET,s_mesh,15
    *SET,st_ang,(f_ang/4)*2
    *SET,ft_mesh,2
    *SET,l_mesh,25
  *ENDIF
  *DO,jj,1,3.5,0.5
    *SET,rad_in,jj
    /INPUT,endmill_model,inp
    /INPUT,endmill_work,inp
    /OUTPUT,parameter_study,txt,,APPEND
    *VWRITE,f_num,rad_in,work
    (F7.0,3X,F16.9,3X,F16.9,3X)
    /OUTPUT
  *ENDDO
*ENDDO
```

APPENDIX E
ANSYS INPUT FILE 04

```
!-----------------------------------------------------------------------------------------
!   ANSYS input file to solve the endmill model. This input file is used
! in endmill_run.inp and endmill_start.inp
!
!                                                                    Dongki Won
!-----------------------------------------------------------------------------------------
PARSAV
/CLEAR
PARRES

/FILNAME,endmill,1
/UNITS,MPA
/TITLE,Damping Design of Endmill
/prep7
!--------------------------------------------------------------------
! Element Type and Material Properties
!--------------------------------------------------------------------
ET,1,SOLID95                !- 20-Nodes Cubic Element
MP,EX,1,206800              !- Modulus of Elasticity : 206780[MPa]
MP,DENS,1,7.82e-9           !- Mass Density : 7.82e-6[kg/mm^3]
MP,NUXY,1,0.29              !- Poisson's Ratio : 0.29
MP,MU,1,0.15                !- Friction Coefficient : 0.15
!--------------------------------------------------------------------
! Create Model Geometry
!--------------------------------------------------------------------
!= Shank:contact surface is 3, 8
K,1,0,0,0
K,2,0,0,1
K,11,rad_out2,0,0
K,12,rad_out1,0,0
K,13,rad_out1,0,101.6
K,14,rad_out2,0,101.6
A,11,12,13,14
VROTAT,1,,,,,,1,2,360,2

!= Finger:contact surfaces are 13,19,25,31,37
*DO,i,1,f_num,1
CYLIND,rad_in,rad_out1,101.6,,st_ang+f_ang*(i-1),st_ang+f_ang*i
*ENDDO
```

```
!-----------------------------------------------------------------
! Generating Mesh
!-----------------------------------------------------------------
LSEL,S,LENGTH,,101.6
LESIZE,ALL,,,l_mesh

vsel,S,volu,,1,2,1,1
LSEL,R,RADIUS,,rad_out1
LSEL,A,RADIUS,,rad_out2
LESIZE,ALL,,,s_mesh
LSEL,S,LENGTH,,rad_out1
LESIZE,ALL,,,st_mesh

vsel,S,volu,,3,3+f_num,1,1
LSEL,R,RADIUS,,rad_out1
LSEL,A,RADIUS,,Rad_in
LESIZE,ALL,,,f_mesh
LSEL,S,LENGTH,,rad_out1-rad_in
LESIZE,ALL,,,ft_mesh
AllSEL

MSHAPE,0,3D                 != hexahedral-shaped elements,3D
MSHKEY,2                    != Map meshing
VMESH,ALL
!-----------------------------------------------------------------
! Designating Contact Pairs
!-----------------------------------------------------------------
ET,2,TARGE170
ET,3,CONTA174
ASEL,S,,,3,8,5,1
NSLA,S,1
ESLN,0
TYPE,2
ESURF,,TOP
ASEL,S,,,13,13+(f_num-1)*6,6,1
NSLA,S,1
ESLN,0
TYPE,3
ESURF,,TOP
FINISH

/SOLU
!-----------------------------------------------------------------
! Apply Boundary Conditions and Sove
!-----------------------------------------------------------------
NSEL,S,LOC,Z,0
```

```
D,ALL,ALL
ALLSEL
SOLCONTROL,ON

! Load Step 1
OMEGA,0,0,2722.713,0
TIME,1
NROPT,UNSYM
NSUBST,5,10,2
AUTOTS,OFF
OUTRES,BASIC,ALL
KBC,0
LSWRITE,1

! Load Step 2
CSYS,1
NSEL,S,LOC,Z,101.6
NSEL,R,LOC,X,rad_out2
NSEL,R,LOC,Y,90
F,ALL,FY,-25
*DO,kk,1,2
  NSEL,S,LOC,Z,101.6
  NSEL,R,LOC,X,rad_out2
  NSEL,R,LOC,Y,90+(360/(s_mesh*4))*((-1)**kk)
  F,ALL,FY,-25
*ENDDO
*DO,kk,1,2
  NSEL,S,LOC,Z,101.6
  NSEL,R,LOC,X,rad_out2
  NSEL,R,LOC,Y,90+(360/(s_mesh*4))*2*((-1)**kk)
  F,ALL,FY,-12.5
*ENDDO
CSYS,0
ALLSELL
TIME,2
NROPT,UNSYM
NSUBST,5,10,2
AUTOTS,OFF
OUTRES,ALL,ALL
KBC,0
LSWRITE,2
LSSOLVE,1,2,1

FINISH
```

APPENDIX F
ANSYS INPUT FILE 05

```
!-------------------------------------------------------------------------------
!   ANSYS input file to calculate the work done by the frictional force.
! This input file is used in endmill_run.inp and endmill_start.inp
!
!                                                          Dongki Won
!-------------------------------------------------------------------------------
/POST1
SET,1,1
ESEL,S,ENAME,,174
*GET,emin,ELEM,0,NUM,MIN
*GET,emax,ELEM,0,NUM,MAX
*GET,aa,ELEM,emin,VOLU
aa=aa*0.25
!-------------------------------------------------------------------------
! Read Friction Stress of R and S direction in each elements
!-------------------------------------------------------------------------
ETAB,taur1,SMISC,5
ETAB,taur2,SMISC,6
ETAB,taur3,SMISC,7
ETAB,taur4,SMISC,8
ETAB,taus1,SMISC,9
ETAB,taus2,SMISC,10
ETAB,taus3,SMISC,11
ETAB,taus4,SMISC,12
!-------------------------------------------------------------------------
! Calculate Friction Force of R and S direction by multiplying area
!-------------------------------------------------------------------------
SMULT,rforce1,taur1,,aa
SMULT,rforce2,taur2,,aa
SMULT,rforce3,taur3,,aa
SMULT,rforce4,taur4,,aa
SMULT,sforce1,taus1,,aa
SMULT,sforce2,taus2,,aa
SMULT,sforce3,taus3,,aa
SMULT,sforce4,taus4,,aa
!-------------------------------------------------------------------------
! Read Slide(Relative Displacement) of R and S direction in each elements
!-------------------------------------------------------------------------
ETAB,tasr1,NMISC,17
```

```
ETAB,tasr2,NMISC,18
ETAB,tasr3,NMISC,19
ETAB,tasr4,NMISC,20
ETAB,tass1,NMISC,21
ETAB,tass2,NMISC,22
ETAB,tass3,NMISC,23
ETAB,tass4,NMISC,24
!-------------------------------------------------------------------------------
! Calculate the work done by the friction force in each elements.
!-------------------------------------------------------------------------------
VDOT,work1,rforce1,sforce1,,tasr1,tass1
VDOT,work2,rforce2,sforce2,,tasr2,tass2
VDOT,work3,rforce3,sforce3,,tasr3,tass3
VDOT,work4,rforce4,sforce4,,tasr4,tass4
SABS,1
SSUM
*GET,work1,SSUM,,ITEM,work1
*GET,work2,SSUM,,ITEM,work2
*GET,work3,SSUM,,ITEM,work3
*GET,work4,SSUM,,ITEM,work4
work=work1+work2+work3+work4
SABS,0
!-------------------------------------------------------------------------------
! Save the slide value for the next step.
!-------------------------------------------------------------------------------
ETAB,tasr1tmp,NMISC,17
ETAB,tasr2tmp,NMISC,18
ETAB,tasr3tmp,NMISC,19
ETAB,tasr4tmp,NMISC,20
ETAB,tass1tmp,NMISC,21
ETAB,tass2tmp,NMISC,22
ETAB,tass3tmp,NMISC,23
ETAB,tass4tmp,NMISC,24
!-------------------------------------------------------------------------------
! Repeat the procedure until reaches to the last set
!-------------------------------------------------------------------------------
ww=0
*DO,uu,1,2
  *DO,vv,1,5
    *IF,uu,EQ,1,AND,vv,EQ,1,CYCLE
    SET,uu,vv
    ww=ww+1
    !-----------------------------------------------------------------------------
    !   Read Friction Stress of R and S direction in each elements
    !-----------------------------------------------------------------------------
    ETAB,taur1,SMISC,5
```

```
ETAB,taur2,SMISC,6
ETAB,taur3,SMISC,7
ETAB,taur4,SMISC,8
ETAB,taus1,SMISC,9
ETAB,taus2,SMISC,10
ETAB,taus3,SMISC,11
ETAB,taus4,SMISC,12
!--------------------------------------------------------------------------------
!  Calculate Friction Force of R and S direction by multiplying area
!--------------------------------------------------------------------------------
SMULT,rforce1,taur1,,aa
SMULT,rforce2,taur2,,aa
SMULT,rforce3,taur3,,aa
SMULT,rforce4,taur4,,aa
SMULT,sforce1,taus1,,aa
SMULT,sforce2,taus2,,aa
SMULT,sforce3,taus3,,aa
SMULT,sforce4,taus4,,aa
!--------------------------------------------------------------------------------
!  Read Slide(Relative Displacement) of R and S direction in each elements
!--------------------------------------------------------------------------------
ETAB,tasr1,NMISC,17
ETAB,tasr2,NMISC,18
ETAB,tasr3,NMISC,19
ETAB,tasr4,NMISC,20
ETAB,tass1,NMISC,21
ETAB,tass2,NMISC,22
ETAB,tass3,NMISC,23
ETAB,tass4,NMISC,24
SMULT,tasr1tmp,tasr1tmp,,-1
SMULT,tasr2tmp,tasr2tmp,,-1
SMULT,tasr3tmp,tasr3tmp,,-1
SMULT,tasr4tmp,tasr4tmp,,-1
SMULT,tass1tmp,tass1tmp,,-1
SMULT,tass2tmp,tass2tmp,,-1
SMULT,tass3tmp,tass3tmp,,-1
SMULT,tass4tmp,tass4tmp,,-1
SADD,tasr1,tasr1,tasr1tmp
SADD,tasr2,tasr2,tasr2tmp
SADD,tasr3,tasr3,tasr3tmp
SADD,tasr4,tasr4,tasr4tmp
SADD,tass1,tass1,tass1tmp
SADD,tass2,tass2,tass2tmp
SADD,tass3,tass3,tass3tmp
SADD,tass4,tass4,tass4tmp
```

```
    !-------------------------------------------------------------------------------
    !   Calculate the work done by the friction force in each elements.
    !-------------------------------------------------------------------------------
    VDOT,work1,rforce1,sforce1,,tasr1,tass1
    VDOT,work2,rforce2,sforce2,,tasr2,tass2
    VDOT,work3,rforce3,sforce3,,tasr3,tass3
    VDOT,work4,rforce4,sforce4,,tasr4,tass4
    SABS,1
    SSUM
    *GET,work1,SSUM,,ITEM,work1
    *GET,work2,SSUM,,ITEM,work2
    *GET,work3,SSUM,,ITEM,work3
    *GET,work4,SSUM,,ITEM,work4
    work=work+work1+work2+work3+work4
    SABS,0
    !-------------------------------------------------------------------------------
    !   Save the slide value for the next step.
    !-------------------------------------------------------------------------------
    ETAB,tasr1tmp,NMISC,17
    ETAB,tasr2tmp,NMISC,18
    ETAB,tasr3tmp,NMISC,19
    ETAB,tasr4tmp,NMISC,20
    ETAB,tass1tmp,NMISC,21
    ETAB,tass2tmp,NMISC,22
    ETAB,tass3tmp,NMISC,23
    ETAB,tass4tmp,NMISC,24
  *ENDDO
*ENDDO
FINISH
```

# REFERENCES


1. Boresi, A.P., Schmidt, R.J. and Sidebottom, O.M., Advanced Mechanics of Materials, fifth Edition, John Wiley & Sons, Inc., NY, 1993.

2. Cobb, W.T., "Design of Dampers for Boring Bars and Spindle Extensions," Master's Thesis, University of Florida, 1989.

3. Dean, M.R., "Improving Milling Efficiency Through Chatter Suppression and Increased Axis Feedrates," Master's Thesis, University, 1998.

4. Schmitz, T., "Predicting High-Speed Machining Dynamics by Substructure Analysis," Annals of the CIRP, 49(1), 2000, pp. 303-308.

5. Slocum, A.H., Precision Machine Design, Prentice Hall, Inc., Englewood Cliffs, NJ, 1992.

6. Smith, K.S., "Chatter, Forced Vibrations, and Accuracy In High Speed Milling," Master's Thesis, University of Florida, 1985.

7. Sterling, Robert A., "Damping of Long Endmills," Master's Thesis, University of Florida, 1989.

8. Tlusty, J., Manufacturing Processes and Equipment, Prentice Hall, Inc., Upper Saddle River, NJ, 2000.

9. Zhong, Z.H., Finite Element Procedures for Contact-Impact Problems, NY, Oxford University Press, 1993

# BIOGRAPHICAL SKETCH

Dongki Won was born May 5, 1972. In February 2000, he received a bachelor's degree with high honors in mechanical engineering from the Dongguk University in Seoul, Korea. In September 2001, he began graduate study in the Department of Mechanical and Aerospace Engineering at the University of Florida. At the time of writing, he is in his last semester at the University of Florida, after which he will start working on a PhD in the Department of Mechanical and Aerospace Engineering at the University of Florida.